Apr 1st, 8:00 AM

Instrumentation for a Mars Entry Experiment

L. Wolfert
Martin Marietta Corporation, Denver, Colorado

M. Kardos
Martin Marietta Corporation, Denver, Colorado

J. Dougherty
Martin Marietta Corporation, Denver, Colorado

J. Cox
Martin Marietta Corporation, Denver, Colorado

INSTRUMENTATION FOR A MARS ENTRY EXPERIMENT

L. Wolfert, M. Kardos, J. Dougherty, J. Cox
Martin Marietta Corporation, Denver, Colorado

Summary

This paper is based on a preliminary design of an entry science package for a Voyager Mars entry and landing capsule. The introduction outlines the various conditions under which the instruments must operate and the range of anticipated measurement parameters. The following sections describe the technology survey, alternative measurement concepts considered, and the instruments selected for the entry science package. The last section is devoted to the complete subsystem operation, sequence of events, data handling, and the system of backup measurements.

Introduction

Mission Constraints

Exploration of the planet Mars has been proposed as a major objective of the space program. Measurements of basic atmospheric parameters will not only provide a better understanding of the natural phenomena on Mars, but they will also help to optimize the design of future Martian landers.

The described entry science package is based on a preliminary design of a Voyager Mars entry and landing capsule completed by the Martin Marietta Corporation for the Jet Propulsion Laboratory under Contract 952001 during the period from June through August of 1967.

The described entry science package for atmospheric measurements is intended for a space capsule that separates from a spacecraft orbiting the planet Mars (Fig. 1). The space capsule decelerates and makes a soft landing on the planet's surface. After separation from the spacecraft and capsule deorbit, entry deceleration from a velocity of about 15,000 fps at an entry angle between 13 and 16 degrees is achieved by aeroshell, parachute, and retrorockets. All measurements will be conducted at altitudes below 800,000 feet. At least 5×10^6 bits of science data can be transmitted during entry and descent. High confidence in the measurement method and extreme reliability of the instrumentation are essential for such a space mission.

All equipment must undergo heat sterilization and must withstand the Saturn V launch and all other mission environments. An additional constraint is that the entry science package contain at least 45 pounds of science instruments[1].

Atmosphere Structure and Composition

Figure 2 shows, besides some ranges of capsule flight conditions, the approximate ranges of atmospheric pressure (P), density (ρ), temperature (T), and composition predicted for Mars. The lower atmosphere structure is essentially described by these parameters. Composition yields the mean molecular weight ($\bar{M}$), which is essential in tying together the structure parameters ($P = \rho TR/\bar{M}$), R being the universal gas constant.

For the Martian exosphere, temperatures as high as 1500°K have been suggested[1,2]. Above a 60-kilometer altitude, a change in composition caused by photodissociation is anticipated. Therefore, atomic oxygen and carbon monoxide may occur in the upper Martian atmosphere also[3]. Atmospheric water vapor of $(14 \pm 7) \times 10^{-4}$ gr/cm^2-column has been reported[4]. Mariner IV measurements indicated a peak ionization near a 120 kilometer altitude.

It was assumed that atmospheric pressure, density, and temperature profiles must be measured with a precision on the order of ±1 percent. Measurement of major constituents and humidity was also anticipated. A mass spectrometer capable of covering a mass range of 10 to 60 within 2 seconds, an accelerometer triad, and pressure and temperature transducers operating at Mach 5 or less were stipulated.

Humidity and other minor constituents can cause important natural phenomena. The importance of the density profile to both engineering and science emphasizes the need for redundant techniques and backup modes. Composition measurements at both low and high altitudes significantly improve atmospheric models and add a degree of functional redundancy.

Trajectory Reconstruction

Evaluation of the various entry measurements to achieve the best atmosphere reconstruction requires consideration of instrument accuracies and response times, equations of motion, and aerodynamics, etc. Statistical techniques such as the Kalman-Bucy minimum variance (linear filter) approach[5] can be applied to computer evaluation. This approach showed good results in the PRIME program. Reference 6 describes an analysis for determining the atmosphere structure, the mean molecular weight, the velocity/altitude history, and the flight path angle history of a descending probe in a low-speed flight from onboard measurements of pressure, temperature, and acceleration.

Surface Imaging

Surface imaging has very high priority and provides the largest amount of data. The objective of the television experiment is to obtain resolution identifiable with orbiter TV down to 1 meter/optical line pair. The camera axis must be parallel to the capsule roll axis. A TV approach using dual 1 inch vidicons with 200 x 200 picture elements, 6 bits/element was stipulated. The Mariner IV Mars flyby supplied data indicating that the mean highlight illumination of Mars was 5 to 7.27 lumens/cm^2 for aphelion and perhielion conditions, respectively, and that the Martian albedo varied between 0.15 and 0.235[7].

Instrument Selection

Technology Survey

The technology base for atmospheric structure and composition measurements has evolved from research and development associated with aircraft, missiles, entry of ballistic payloads and manned satellites, satellite orbit decay, high-altitude atmospheric observations from balloons, drop sondes, rockets and satellites, and trajectory reconstruction for lifting body and planetary entry vehicles. The technology supporting the surface imaging is based on development carried out for the Rangers, Mariner IV, Mariner 1969, and ESSA (automatic picture taking system) programs, as well as vidicon sterilization programs.

The aerodynamic flow regime of the Martian entry and descent are shown in Figure 3. The most significant parameters are speed and density or mean free-path length. The speed will be hypersonic to an altitude below 100,000 feet and, for practical purposes in designing the entry science experiments, it can be called hypersonic almost down to parachute deployment. In the molecular flow regime, the Knudsen number is large and satellite experiment technology can be applied. During part of the entry phase, the capsule itself may be in continuous flow while a small protruding probe is not. During hypersonic and supersonic continuous flow, the high speed is the primary effect. Above Mach 5, density can be accurately measured, but other atmospheric measurements are difficult unless the instrument senses the atmosphere beyond the shock layer. As the velocity decreases below Mach 5, direct measurements of basic atmospheric parameters become more accurate. After parachute deployment, the capsule rapidly approaches subsonic speeds or is subsonic. For this range, the technology is quite mature and measurements can be made with good confidence. Installation geometry of instruments on the capsule structure can be refined by wind tunnel tests.

After the basic measurement and data handling concepts were established in the initial Voyager study phase, specific instruments were chosen. To achieve a good selection, a thorough search of existing relevant instrument technology was conducted[8-11]. This search included review of technical literature, information reported on instruments used in other high altitude and space programs, and a survey of vendor descriptive information. About 70 instrument manufacturers were contacted during instrument selection.

Alternative Measurement Concepts

General Considerations. Generally, the atmospheric sensors must be directly exposed to the atmosphere in front of the entry vehicle where the aerodynamic conditions are relatively well defined or can be calibrated, and where the ambient gas is not significantly contaminated by the entry capsule. However, to reduce capsule bus weight, the aeroshell in front of the lander must be separated and discarded as soon as its decelerator function is completed. During the study, it became apparent that a group of instruments should be mounted on the aeroshell. The disadvantages of some instrument duplication were outweighed by the advantages of simple, reliable, lightweight electrical connections to the aeroshell instruments, better measurement conditions, and instrument specialization for the entry phase. Therefore, one group of instruments was specifically selected for the hypersonic and supersonic entry phase before parachute deployment. Another group of instruments is mounted on the lander and performs some entry and all terminal descent and landing experiments.

Many techniques for atmospheric measurement have been proposed, investigated, or applied. The large number of attempts is due to the lack of satisfactory instruments for a wide range of applications. Only a relatively small number of possible measurement techniques are outlined in Table 1. Some of the major considerations for instrument selection or rejection are pointed out. The following descriptions refer to the various columns of Table 1.

Density From Acceleration Measurements (Column 1). Determining atmospheric density from deceleration measurements requires an accurate knowledge of velocity and the ballistic coefficient. This coefficient is influenced by vehicle angle of attack, composition, velocity, and the vehicle mass change caused by fuel consumption. The drag coefficient can initially be determined for various anticipated atmospheres. After the space mission, the environment can be more exactly simulated.

Density from Stagnation Pressure Measurement (Column 2). Accelerometers are generally more accurate than pressure transducers; however, a higher density accuracy is expected from the stagnation pressure measurements. During entry, the high speed itself exerts the primary effect on measurements in the range before parachute deployment. For example, the dynamic pressure ($1/2\,\rho V^2$) is much greater than the static value; the ratio being $1/2\,\gamma M^2$ (γ = ratio of specific heats, M = Mach number, ρ = mass density, and V = velocity). Thus, although the pressure at the stagnation point on the vehicle is affected by the ambient atmosphere and gas chemistry, such a measurement really yields the dynamic pressure. The effect of the various flight regimes -- continuum, transition, and free molecule -- is only to modify the corrections of the dynamic pressure measurement required. The measurement remains one of dynamic pressure. The same argument applies to the temperature (or enthalpy). The stagnation enthalpy is essentially $1/2\ V^2$, the freestream static enthalpy being a small fraction of this value.

The dynamic pressure $1/2\ \rho_\infty V_\infty^2$ and stagnation point pressure P_s are related by

$$\frac{P_s}{\rho_\infty V_\infty^2} = 1 + \frac{1}{\gamma M_\infty^2} - \frac{\rho_\infty}{2\,\rho_2} \quad \text{for continuum flow}$$

$$= 1 + \frac{1}{\gamma M_\infty^2} + \frac{1}{M_\infty}\sqrt{\frac{T}{2\gamma}\,\frac{T_r}{T_i}} \quad \text{for free molecular flow}$$

where ρ_2/ρ_∞ is the density ratio across the normal shock and T_r/T_i is the temperature ratio of the reflected and incident molecules. Romeo has shown (Ref. 22) that the right side of this equation is remarkably constant (near 0.96) even for low supersonic Mach numbers. In the transition range, some theory exists (see, for example, Ref. 23) but experimental correlation is needed (Ref. 24). The important point is again made that the effect of various flight regimes on gas composition is a relatively small correction (the right side of the equations above is near unity if M is large). A reasonable approximation to those effects will lead to an accurate evaluation of $\rho_\infty V_\infty^2$ and, hence, of the density. It is assumed that the trajectory reconstruction has yielded the velocity.

Density Measurement with Radiation Gages (Columns 3,4,5,6,7). Density measurement by particle backscatter or absorption of alpha, beta or gamma rays is very interesting because with these techniques one can reach beyond the shock layer of the vehicle. Alpha and beta particles have been used for high atmospheric densities, while electrically generated X-Rays and electron beams have been applied for low-density regions. Ref. 26 describes alpha and beta absorption gages for densities above 7×10^{-4} and 10^{-6} gr/cc, respectively. Beta ray forward scatter (Column 4) has been applied for density measurements above 10^{-7} gr/cc. In the density range from about 4×10^{-8} to 4×10^{-13} gr/cc, the atom density can be measured by sensing the number of "brems strahlung" X-Ray photons generated by the electron beam and radiated to the X-Ray detector (see Column 6). This measurement is influenced by the type of atoms (composition).

Scattering of gamma and X-Rays is useful for densities above 5×10^{-10} gr/cc. The radiation source can be a radioisotope, though electrical sources such as an X-Ray tube may cause less interference because they emit only when energized. However, electrical X-Ray sources may require more weight than radioisotopes. The effects of Compton scattering or photoelectric absorption, followed by fluorescence (emission of a characteristic X-Ray), are used for density detection.

Table 1, Column 7, shows the instrument concept for a density sensor utilizing the technique of electron beam-induced luminosity. This method is advantageous because the gas can be sensed in a region where it will not be aerodynamically disturbed while partial density and composition are measured. The composition measurement is based on the luminosity at specific optical spectra that are characteristic for various anticipated constituents. The light intensity is a measure of the partial density. Development of this promising method is incomplete, but, if perfected, it may provide density and composition data concerning the undisturbed atmosphere several orders higher than possible with the open ion source mass spectrometer.

Measurements With and Modifications of Langmuir Probe (Column 8). Langmuir probes and modified Langmuir probes measure currents caused by ambient electrons or ions. These currents are a measure of the ambient electron or ion density. The particle polarity and the kinetic energy relative to the detector can be determined by application of "potential hills" generated by electrical grids in front of the collector. The thermal electron velocity is generally higher than spacecraft velocity. However, the thermal velocity of the much heavier ions is usually a small fraction of the spacecraft velocity. Therefore, the potential hill primarily senses the electron temperature while the ion measurements primarily yield the molecular weight because ion kinetic energy is mainly caused by the satellite velocity. The ion temperature can also be deduced from the spread of kinetic energies for one constituent [30-32,100, 101]. Measurements with a modified Langmuir probe would yield significant information about charged particles, but electron density can also be obtained from spacecraft occultation experiments. For the early Martian entry measurements, higher priority was given to other experiments.

Composition from Absorption Spectra (Column 9). Scanning the atmospheric absorption spectra from infrared to ultraviolet would provide much information about the atmospheric composition versus altitude. However, the heavy instrumentation and large data rate required for a spectrometer are not necessary because essential information can be obtained from measurements with filters in various selected absorption bands. A field of view of 2π steradian can be achieved with an opalescent and/or diffusing light collector. Then no sun pointing is necessary. Different light detectors (photomultipliers with selected photocathode materials for UV, specific semi-conductors for IR are necessary to sense radiation that passes the selected filters. The following absorption bands have been proposed[33]: 0.28 μ for O_3, 1.6 μ for CO_2, 1.87 μ for H_2O. Because a mass spectrometer provides a much wider range of unambiguous composition and density measurements, this instrument appears preferable, unless the small weight of a multichannel radiometer is most important. However, an absorption radiometer can provide valuable composition information in addition to the molecular weight measurements of a mass spectrometer.

Emission Spectroscopy (Column 10). During the high-speed entry phase of a space vehicle, the shock layer temperature can reach several thousand degrees Kelvin. Due to these high temperatures, the gas can be excited to produce optical radiation spectra that are characteristic for the atmospheric composition. Possible interference from the ablator material must be considered. The ratios between specific constituents and their densities may be determined by observing radiation in selected wavelength bands with a combination of optical filters and detectors. Theoretical and experimental work in shock-layer radiation from proposed planetary atmospheres has been reported in References 41, 48 and 51. These have dealt with both equilibrium and nonequilibrium gas dynamic states in the stagnation region of entering vehicles. Unfortunately, most of these studies applied to emission spectroscopy at high-velocity entries, with stagnation temperatures greater than 5000°K [41-51]. For the investigated application, temperatures between 2000 and 3000°K are more likely to be encountered. Thus, emission measurements would probably have to be restricted to the infrared region of the spectrum.

In the infrared region there is a CN band system near 1 μ, a CO_2 band at 4.3 μ, a CO band at 4.8 μ, and an NO band at 5.3 μ. With the proper choice of filters, or preferably the use of a scanning or multichannel low-resolution spectrometer, composition data could be obtained by continuously monitoring the CN band systems for relative intensities among these species. However, the limited number of bands in the infrared region makes this shock-layer technique too expensive for the limited information it provides.

Mass Spectrometer Measurements During Entry. To understand the structure and influence of the Martian atmosphere, it is important to know its composition, including the minor constituents. Minor constituents can cause considerable solar absorption, or offer possible clues to the planet's physical nature, history, or biology. Hence it is desirable to apply measurement techniques that can detect small amounts of stable and uncontaminated reactive gases. From the altitude rate of change of the ratio of any two constituents of different mass, the gas temperatures can also be calculated under the following assumptions[52]:

1) The two constituents are in thermal and diffusive equilibrium under the influence of the gravitational field;

2) Activity resulting in chemical changes of the constituents is absent or negligible.

Under these conditions, temperature is given by the relation

$$T = \left[(g/R) \quad (M_2 - M_1)\right] \Big/ d/dz \ln (n_1/n_2)$$

where

T = temperature, °K

g = acceleration due to gravity, cm/sec^2

R = universal gas constant = 8.3146×10^7 ergs $deg^{-1}K$ gm $mole^{-1}$

M = molecular weight of the constituent

z = altitude, cm

n = number density of the constituent

Mass spectrometry is an obvious choice for composition and density measurements. The atomic or molecular weight is determined by ionizing the gas and separating the ions according to their mass by magnetic and/or electrostatic fields. With this method, the pressure may be as low as 10^{-12} millibar (10^{-18}gr/cc) and a mass spectrum of about 50 atomic mass numbers can be analyzed within two seconds or less. Mass spectrometers without ion source are applied to measure ion composition. Especially for high-altitude measurements in the molecular flow region, surface reactions as well as absorption and desorption of the walls must be avoided as much as possible. Fortunately, mass spectrometers at high altitudes can be "open" to the atmosphere and do not require inlet leaks to maintain an analyzer pressure below 5×10^{-4} millibar. With the "open" mass spectrometer, surface interactions can be avoided and such ion composition and reactive neutral constituents as atomic oxygen can be analyzed.

Mass Spectrometer in Cavity (Column 11). Mass spectrometers in a cavity take advantage of the density enhancement factor of about 40 and increase the measurement altitude. The density increase in front of the aeroshell is due to the capsule bus entry velocity. However, when the density changes very rapidly during entry (doubling every two seconds), the walls will act as effective pumps or sources of molecules due to absorption, desorption, and replacement effects[53, 54]. These difficulties would also influence any free-molecule-impact pressure gaging system. Another source of composition errors are surface reactions of reactive gases[55]. To evaluate the conditions for transition flow, low-density wind tunnel modeling would probably be needed.

Flythrough Mass Spectrometer (Column 12). The flythrough mass spectrometer is designed to overcome difficulties anticipated for cavity mounting. A molecular beam is generated out of the freestream gas, utilizing the vehicle motion to produce an extremely high vacuum in the region surrounding the beam. This approach was not selected for application because it requires a relatively heavy deployment mechanism and has not yet been tried.

Open Ion Source Mass Spectrometer (Column 13). Open ion source mass spectrometers, carried by rockets and satellites, have been utilized for atmospheric composition and density measurements for about six years[56]. The ion source is projected into the gas medium and surface interactions are minimized. A novel ion source modification, originally suggested by Southwest Research Institute, would add a repeller grid to the open ion source. All particles except those with freestream relative potential energy can be excluded by means of a potential hill that is roughly M x V/75 volts (M molecular weight, V - space capsule velocity in km/sec). By applying this repeller potential periodically, the portion of analyzed freestream particles can be determined by composition and density. The open ion source mass spectrometer, periodically utilizing a repeller grid, was chosen for high-altitude measurements although investigations are needed to develop and calibrate it.

Molecular Speed Ratio Probe (Column 14). At a high enough altitude, the Knudsen number ($Kn = \lambda/L$, λ = mean free path, L = characteristic length of configuration) is too large for continuum devices to be useful. For that regime, the free molecular speed ratio probe described by Vidal, Skinner, and Bertz[60] may be appropriate. The instrument measures two heat transfers. The ratio of stagnation point to flat plate heat transfer for a zero angle of attack is, for free molecule flow, just the molecular speed ratio (ξ)

$$\xi = V \Big/ \sqrt{\frac{2\ RT}{M}}$$

where R is the universal gas constant and M the ambient molecular weight. Determination of V from reconstruction of the trajectory with this molecular speed ratio then yields the ambient, translational (static) temperature T. On the other hand, simply by substitution of the perfect gas equation of state, this ratio may be written as

$$\xi = \sqrt{\frac{1/2\ \rho V^2}{P}}$$

Then since the dynamic pressure ($1/2 \rho V^2$) is found separately from pitot pressure or deceleration, the speed ratio will yield the ambient pressure P.

Vidal has shown that the probe behavior is satisfactory for Knudsen numbers, greater than about 7, based on gage dimensions. He has also estimated performance for probe dimensions of about 0.016 inch, which would allow operation to as low as about 140,000 feet, depending on the atmosphere. Further, the theory is such that composition uncertainties should not directly influence performance.

There are several new considerations that will arise in the Voyager experiment that have not been considered in the existing speed-ratio probes. For example, the existing probes are used in only short-duration experiments, while the Voyager experiment will last for several minutes. Therefore, provisions will be required to cool the instrument. Similarly, provisions will be required to maintain a surface with known accommodation coefficients during the space flight. These do not present any basic difficulty and can be accomplished with existing technology.

Ambient Pressure from Multiple Pressure Measurement (Column 15). Theoretically it appears possible to derive ambient pressure from two or more different pressure measurements on the entry capsule. The ambient pressure P_∞ is related to the two pressure measurements P_1 and P_2 by the relationship

$$P_\infty = P_2 \frac{C_{P1} - C_{P2} \quad P_1/P_2}{C_{P1} - C_{P2}}$$

where C_{P1} and C_{P2} are pressure coefficients that are a function of atmosphere composition, Mach number, and possibly Reynolds number. It is at least very difficult to simulate all these conditions in model tests and to determine the pressure coefficients with sufficient accuracy. Probably one pressure measurement should be taken on the vehicle base to get the maximum difference between pressures. Perhaps a single base pressure measurement can be closely related to ambient pressure. However, the feasibility of this method remains to be demonstrated. The argument against this theory is that no gas will reach the blunt flight capsule surface without going through a very strong shock, which essentially erases its memory of free stream conditions. However, the possibility that multiple pressure measurements or the base pressure would, in fact, be well correlated to ambient pressure cannot be dismissed entirely. The simplicity of such a measurement is most attractive.

Sideport Pressure Probe (Column 16). To be useful, the sideport pressure probe must not seriously degrade the aerodynamic stability or introduce a significant degradation in the aeroshell drag. Numerous problems are involved in deriving ambient pressure from these measurements in the free molecular flow regime at hypersonic entry velocities.

However, for the lower part of the atmosphere, a conventional static probe consisting of a spherically blunted cylinder with static ports well back from the nose is appropriate. As the high heating regime is approached, the rounded nose will minimize peak heating. Such probes have already been extensively evaluated[64-66], and the correlation data obtained are good on the basis of the hypersonic interaction parameter.

The use of such a probe requires correlation of its performance through large values of the hypersonic interaction parameter ($M^3 / \sqrt{Re}$). Insensitivity to atmospheric composition is important. Because of the substantial shock standoff distance, such a probe must be several feet long. A minimum length at which the main shock on the aeroshell does not interfere with probe behavior must be determined experimentally.

Because of the difficulties caused by the low Reynolds number and attendant possible separation and/or boundary layer thickening, application of a sideport pressure probe before aeroshell separation was considered premature. However, development should be pursued because of the lack of a demonstrated alternative for directly measuring ambient pressure.

During terminal descent after parachute deployment, the entry vehicle will be descending through the atmosphere at subsonic velocities. The measurement environment during this period is characterized by continuum flow and shock effects are absent. Here the technology is quite mature, and measurements can be made with good confidence. Installation geometry of instruments on the capsule structure, after release of the aeroshell, can be refined by wind tunnel tests.

At subsonic speeds, the aerodynamic flow field extends far ahead of the lander, and ideally the sideport pressure tube should be several times as long as the lander to avoid aerodynamic disturbances. This is not very practical. Sideport pressure probes of practical length could be calibrated by wind tunnel testing of the lander configuration. However, during parachute descent the lander velocity decreases rapidly to Mach 0.4 and below. Under these conditions the total pressure is less than 15 percent above ambient pressure ($P_t = P_s\left[1 + \frac{\gamma - 1}{2} M^2\right]^{\frac{\gamma}{\gamma - 1}}$). The velocity is accurately determined by radar and the influence of the anticipated range of gas composition and temperature is small (see stagnation pressure measurement). However, these parameters will also be measured.

Because of the above considerations, as well as the weight, complexity, and aerodynamic simulation requirements, application of a sideport pressure probe was not believed justified and this probe was not selected.

Total Pressure Measurement (Column 17). Total pressure measurement methods during terminal descent are relatively simple and are based on a well-established technique. A short "shielded" pitot tube (see Figure 7) is directed into the flow.

The pitot tube shield makes the probe insensitive to large (±30 degree) angles of attack. Over most of the terminal descent range (velocity < Mach 0.4), the total pressure is less than 15 percent above the ambient pressure. Ambient pressure can be quite accurately computed from total pressure and has been described in the discussion of sideport pressure probe applications.

Radiation Thermometer (Column 18). The total energy radiated from a black body is proportional to the fourth power of its absolute temperature and the spectral distribution is also a function of temperature (Wien's displacement law). Although gases are often transparent in the visible spectrum, many atmospheric constituents become absorptive at a number of wavelengths in the IR spectrum. Utilizing this effect, radiation thermometers essentially operate by comparing the amount of radiation emitted by the target with that emitted by an internal, controlled reference source. For gas thermometers, filters usually select the light in a specific absorption band. One such wavelength region is the 15-micron CO_2 band.

The great advantage of radiation thermometers is their ability to remotely sense temperature. At the very low densities experienced during the entry phase, radiation thermometers might be superior to immersion thermometers if the very hot shock layer surrounding the entry vehicle would not cause difficulty in measuring the undisturbed atmosphere. However, for measurements from airplanes, the path traversing the shock waves and boundary layer apparently does not cause serious errors because of the relatively short absorption path length[67]. The radiation thermometer's heavy weight and the instrument's complexity are additional disadvantages. It was not selected for application.

Vortex Thermometers (Column 19). The objective of vortex thermometers is to use adiabatic cooling near the center of an air vortex to compensate for the aerodynamic temperature rise and to obtain ambient temperature near the sensing element. The gas is caused to whirl by a spiral stator vane aligned longitudinally with the flight path. However, extensive testing showed that it was impossible to design one configuration for a wide range of airspeeds and altitudes. Since its extreme sensitivity to angles of attack have limited its application to few research aircraft[69], it appears even less feasible for the wide range of atmospheric parameters during planetary entry.

Immersion Temperature Sensors (Column 20). The state-of-the-art for low-density immersion temperature sensors was significantly advanced during the last decade by their applications in parachute drop sondes for temperature measurements below a 200,000 foot altitude[70, 73]. Measurements with these sensors at low drop velocities are accurate to about 1 percent of absolute temperature at densities above 10^{-6} gr/cc. Difficulties at lower densities are caused by heat transfer to the sensing element by electrical lead wires, and by radiation, aerodynamic, and electrical heating. Table 1, Column 20, shows a mounting with a thermistor sensing element. The thermistor is connected to a 0.0004-inch-thick aluminized Mylar film that has a large surface-to-mass ratio, low heat conduction, and good reflectivity[74]. Thermistors are used for rocket sondes because of their high temperature coefficient. Such immersion sensors appear feasible for the application; however, the aerodynamic heating effects would have to be calibrated and more mechanical protection against damage of the delicate sensor may be necessary.

Total Temperature Probe (Column 21). The total temperature of a gas is achieved when the gas is brought to rest (or nearly so) without removal of any heat. The temperature rise above ambient temperature is caused by the change of relative kinetic gas energy into thermal energy. The total temperature, T_o, is related to the ambient temperature T_∞ by $T_o/T_\infty = 1 + (\gamma - 1) M^2/2$, where γ is the ratio of specific heats and M is the Mach number.

A probe with a recovery factor of one would sense the total temperature exactly. This condition cannot be completely achieved. Some gas flow from the stagnation point to the sensing element is needed and additional errors are caused by heat radiation and conduction effects. Especially for low gas densities corresponding to altitudes of more than 100,000 feet on Earth, no satisfactory commercial total temperature probes are available because most applications are below 70,000 feet. However, utilizing the temperature sensor technology developed for meteorological rocket sondes to a new total temperature probe, development of a probe that will accurately measure temperature at stagnation pressures above 0.5 millibar or densities above 0.5×10^{-6} gr/cc appears feasible. Details of such a probe will be discussed in a later section.

Total temperature probes were selected for velocities below Mach 5 and pressures above 0.5 millibar because satisfactory designs are considered within the state-of-the-art and the performance and requirements compare favorably with other approaches.

At Mach 5, the total temperature is several times the ambient temperature and the probe is less accurate because of the high total temperature. Therefore, large errors in ambient temperature calculations are anticipated at Mach 5. However, these errors decrease rapidly because the total temperature increase is proportional to the square of the Mach number.

Kryptonate and Single-Gas Detectors (Column 22). If a radioisotope such as Kr^{85} (Krypton) can be stably embedded in a solid that reacts with a specific gas, chemical erosion will cause a proportional loss of radioactivity (0.67 Mev betas) and thus provide a measure of the reactive gas. Investigations of such a kryptonate oxygen detector for Mars or Venus are described in References 75 and 76. Detection of 2 ppm is reported when the kryptonated source is heated to 1000°C. However, this approach is in the experimental stage and applications to atmospheric measurements are not known.

Many types of single-gas detectors are being studied for use in the Martian atmosphere[76]. These usually rely on some property or effect (not always unique) of the gas used in their operation. Such methods are not considered suitable for analysis of an unknown atmosphere of possible widely varying composition, at least not in the early stages of exploration. They are, however, very suitable for use as auxiliary experiments to confirm an analysis by mass spectrometry or gas chromatography. The weight of these sensors is on the order of 1 pound.

Gas Chromatography (Column 23). During a gas chromatograph analysis, an atmospheric sample, together with an inert carrier gas, is injected into one or more gas chromatograph columns. The columns contain absorptive material or molecular sieves. As the gas is flushed through the column, the gas constituents take different time periods until they have passed the column and reach the detector. The duration of these time periods is a measure of the composition, and the signal intensity indicates concentration of the specific constituent. Electrical breakdown detectors are mostly applied in airborne gas chromatographs.

Usually gas chromatographs require several minutes for an analysis. Test results of a gas chromatograph column for a few constituents (CO_2, N_2, Ar), with response times of several seconds, have been reported[80]; however, we do not know of a complete Martian gas chromatograph capable of analysis in 10 to 20 seconds. An instrument developed in 1962 requires several minutes for an analysis. Because of the electromechanical parts and/or squibs in a gas chromatograph, mass spectrometers were rated more reliable. A gas chromatograph was not selected because it provides information about preselected constituents only and the analysis of many constituents within a few seconds remains to be demonstrated.

Mass Spectrometer with Inlet Leak (Column 24). Because mass spectrometers operate at pressures below 5×10^{-4} millibar, an inlet leak and pumping action (ion or getter pump, or evacuated volume) are needed. To minimize sample transport lags, the inlet leak must be near the analyzer and a flow much larger than the leak flow is sampled in front of the lander. The sampled gas passes by the leak and is vented to the wake. Internal shocks in the sampling tube should be avoided and turbulent mixing near the leak is desirable. In the mass spectrometer analyzer, several decades of partial pressures can be measured. Measurement of molecular weights below 60 or 100 atomic mass units are considered sufficient for atmospheric analysis. Quadruple mass spectrometers can also indicate whether any constituents above a mass number occur.

The mass spectrometer was selected because it provides, within a few seconds, an analysis of molecular weights yielding composition, and the partial pressure measurements can range over several decades. High reliability is achieved because no moving parts are needed.

Humidity Measurements during Terminal Descent. Data presently available indicate only about 15-micron precipitable water on Mars[4]. At such low humidities, any form of sample transport (sampling tube, etc) tends to change the humidity of the rapidly changing atmospheric samples because of water vapor absorption or desorption on the surface of materials. Therefore, the hygrometer will be deployed into the uncontaminated gas flow.

Dew Point Hygrometer (Column 25). Dew point hygrometers are based on the phenomena of dew or frost formation when a temperature-controlled element decreases to the dew/frostpoint temperature, which depends on the humidity content of the atmosphere. The saturated vapor pressure at this temperature is the partial pressure of water vapor in the atmosphere. Dew point hygrometers have been successfully used for high-altitude atmospheric measurements on Earth. However, thermoelectric coolers are most practical but achieve a temperature decrease of only about 90°C, and the response time at the lowest temperatures is too long. Also, the time required for sufficient frost layer change at low frost points is much longer than 1 second. Other disadvantages are weight (0.7 lb) and power requirements (10 w). The dew point hygrometer was not selected because other approaches are more promising.

Phosphorous Pentoxide Electrolytic Hygrometer (Column 26). The operation of a phosphorous pentoxide electrolytic hygrometer is based on the measurement of a current causing the electrolysis of water vapor absorbed by a sensor or cell containing phosphorous pentoxide. The feasibility of such a hygrometer was investigated[87]; however, because of time effects and material contamination, feasibility for the sterilization and spacecraft environments could not be demonstrated.

Aluminum Oxide Hygrometer (Column 27). Aluminum oxide hygrometers basically consist of an aluminum substrate with an aluminum oxide layer. A porous, but electrically conductive, gold film is evaporated on the aluminum oxide. The hygroscopic aluminum oxide changes its conductance as a function of absolute water vapor concentration; the gold film and the aluminum substrate serve as electrodes. Aluminum oxide hygrometer elements can be very small (1 x 0.4 x 0.003) and their conductance can change between 10^5 and 10^6ohms and is rather independent of pressure and temperature[92]. Measurements over a dew point range from -130°C to +10°C dew/frost point seem possible and initial tests showed encouraging results in regard to environmental stability.

Because of its favorable characteristics, the aluminum oxide hygrometer was selected. Its feasibility should be carefully investigated and tested.

Surface Imaging. Some approaches in addition to conventional television deserve consideration for surface imaging. The requirements for short exposure time to avoid smear, and for sterilizability, high terminal resolution (1 meter), low weight, and low power limit the final choice. The location requirements and tradeoffs are very similar for any surface imaging concept. Three promising locations are shown in Column 28. A camera looking through a window in the apex of the nose cone and mounted to the aeroshell must be discarded at aeroshell separation. If start of imaging after aeroshell separation can be tolerated, then the imaging system can be located at the most convenient location on the lower side of the lander. A lander-mounted imaging system can be used before and after aeroshell staging if a window on the side of the aeroshell is provided; however, a heavy nonablating heat shield between the window and center of the aeroshell is then advisable to avoid contamination of the window.

Tradeoff considerations showed that both wide-angle and narrow-angle cameras were needed. Because high resolution is essential only after aeroshell staging, the narrow-angle field of view camera was mounted on the lander and the wide-angle field of view camera was mounted in the nose of the aeroshell.

Facsimile Camera (Column 28). Facsimile cameras usually have one light detector and optically scan consecutive points of an image[93]. Therefore, long exposure times are needed for one picture. This disadvantage is not acceptable during entry, in spite of the advantages of simple camera design.

Photographic Imaging System (Column 29). A photographic imaging system takes advantage of the very small and highly sensitive elements of a photographic film. However, the photographic film must be processed and scanned electro-optically. This requires not only heavy electromechanical and chemical equipment, but the pictures could not be transmitted before landing because of the long processing period.

Dielectric Tape Camera (Column 30). Dielectric tape, drum, or disc cameras avoid the disadvantages of the photographic process and store the image electrostatically. The information can be read out immediately. Such a camera, developed for NASA, weighed 83 pounds. This weight alone makes it prohibitive for a Voyager-type application in view of the imaging system described in the following section.

Vidicon Camera System (Column 31). Vidicon cameras are based on electrostatic storage of images. The dielectric is photoconductive. All storage elements have one common transparent electrode. The other side of the storage elements consist of many small electrodes that are first discharged due to illumination by the preparation lamp to erase the residual image. Then the storage elements are equally charged by the defocused electron beam. During imaging, the photoconductive dielectric causes a partial discharge of the storage elements, depending on the light intensity. This electrostatic image can be stored for about 30 seconds. For readout, the electron beam scans again at the desired speed and charges the capacitor elements. The charge current provides a measure of the image brightness at the scanned image elements.

Cameras with vidicons are sterilizable, have a good development status, and good performance. The requirements of power and weight are relatively small. A wide-angle vidicon camera was selected for aeroshell mounting and the narrow-angle vidicon camera was planned for lander mounting. This camera starts imaging after aeroshell separation. Camera details are described in one of the later sections.

Discussion of Selected Instruments

Stagnation Pressure Sensor (Aeroshell). During entry, pressure at the aeroshell stagnation point ranges from very low values in the early portions of the trajectory to perhaps 100 millibars at the point of maximum aerodynamic interaction. For this reason, a vibrating-diaphragm gage is selected for one of the transducers to measure stagnation pressure. Its outstanding characteristics are a wide pressure range (10^{-4} to 100 millibar), high accuracy (1 percent of reading) and small size. During measurements, the diaphragm is exposed to pressure on both sides and is vibrated by electrostatic forces. The damping effect on the thin vibrating diaphragm is sensed electrically and used for pressure indication. Because operation is based on viscous effects of the medium being measured, the transducer output is affected by gas composition and temperature. For this reason stagnation pressure is redundantly sensed with an absolute stretched diaphragm gage for a range from 0.5 to 50 millibars. An instrument of this type is not influenced by gas composition and thus provides a measure of the influence of composition on the response of the vibrating diaphragm transducer. The dual measurement by a physically different means also provides functional redundancy in obtaining stagnation pressure data. Figure 4 shows the installation of the pressure transducers in the aeroshell nose and includes specific information concerning performance of the instruments and a functional block diagram of their electronics.

Introducing a phase shift in the cell drive voltage checks out the electronics of the vibrating diaphragm transducer. In the stretched diaphragm transducer, a pressure input is simulated by connecting a capacitor parallel to the diaphragm pickoff. The output of both instruments is measured at entry to determine zero drift of the transducers.

Open Ion Source Mass Spectrometer (Aeroshell). The open ion source mass spectrometer measures number densities of neutral atmospheric species and operates until the ambient pressure exceeds about 10^{-4} millibar. No pump is required because the difference between stagnation and wake pressure ensures flowthrough of analyzed particles (Figure 4). With the open ion source, ambient particles can enter the analyzer without surface interaction. However, the composition of particles that contacted the aeroshell or instrument surface may have been changed before they enter the analyzer. During the in-flight calibration mode, these possibly reactive and contaminated particles are repelled.

After warmup, the instrument receives the start signal at entry and the mass spectrometer sweep begins. Mode control determines whether the mass spectrometer measures peak amplitudes (normal mode) or whether only RF voltages are applied to the quadrupole rods. In the latter case, operation is in the staircase mode. Partial pressure measurements will also be provided. Details of the quadrupole mass spectrometer operation and peak-sensing techniques are given in the later discussion of the terminal descent phase mass spectrometers. Signals from the ion detector are amplified and then digitized. Engineering measurements to check analyzer sweep voltage and frequency, emission current, bias voltages, and heater current are digitized and multiplexed with the digital composition data. For every fifth scan, an in-flight calibration mode will be activated by increasing the potential of the ion source repeller grid to a value slightly more positive than the anode potential to repel particles that do not have free-stream kinetic energy.

Accelerometers. A force balance accelerometer with high performance, demonstrated reliability, lightweight, wide operating temperature range, small size, and lower power requirements was selected. The basic function of a single-axis accelerometer servoloop is shown in Figure 5. A capacitive pickoff detects minute deflections of the proof mass. This signal is amplified and the servoamplifier generates (by means of the force coil) a magnetic force that compensates the acceleration force exerted on the proof mass. The current through the force coil is a measure of the acceleration.

Temperature drifts of scale factor (about 20 ppm/^{o}F) and bias ($< 5\,\mu g/^{o}F$) can be corrected because the triad temperature is measured. The full range of the two accelerometers that sense normal to the flight capsule roll axis is ± 0.5 g. The accelerometer measuring along the roll axis has a full range of 25 g. To increase the accuracy of the acceleration measurement along the roll axis, automatic range switching will be provided. A saturable amplifier will provide a 5 volt output at a 1-g acceleration. Another signal amplifier will provide 5 volts at a 25-g acceleration. If required, higher accuracy can be achieved with more amplifiers and additional steps of range switching.

The accelerometer system can be checked out by simulating an acceleration with a checkout current through the accelerometer force coil. The accelerometer bias errors will be measured under freefall conditions after the electronics are warmed and shortly before atmospheric entry. At least one acceleration measurement is planned after landing to check the accelerometer scale factors.

The block diagram in Figure 5 shows that one preamplifier associated with each accelerometer is part of the accelerometer triad. The accelerometer triad will be mounted near the flight capsule cg. However, the servoamplifiers and the power conditioning units (regulator and power converter) will be in the signal conditioning unit.

Total Temperature Sensor (Aeroshell). Figure 5 shows the concept proposed for the total temperature sensor, which will be mounted in the aeroshell instrument module and exposed at an inertial velocity of about 3000 fps. Three heat shields and reflective thermocouple coatings reduce the radiation error. Relatively long, thin wire (0.002-in) thermocouples are provided to achieve the necessary fast response and temperature equalization between the low-density gas and the sensor. Gas exit ports in the probe provide some flow of the stagnated gas to the thermocouples. These sense the gas temperature along the probe axis to avoid the influence of the tube boundary layer. The use of parallel-connected thermocouples increases the sensor reliability. This instrument will also be able to sense total temperature during terminal descent in case the aeroshell fails to separate. Sensor voltage is corrected with an electrically compensating thermocouple junction before the low voltage is amplified in the low-drift high-gain amplifier. The thermocouple output is on the order of 40 $\mu v/^{o}C$. The performance required of the instrument electronics can be obtained using a chopper-stabilized amplifier. Equipment of this type, with about 30 μv total drift over 6 months and 0.2 $\mu v/^{o}C$ temperature sensitivity, is within the state-of-the-art. The electronic amplifier can be checked by connecting the amplifier input to a calibration voltage. The complete total temperature probe can be checked by measuring the temperature of the radiation shield of the probe when the entry capsule is exposed to free space ($< 10^{-4}$ mb pressure). Then the thermocouples assume the temperature of the radiation shield. Knowledge of the radiation shield temperature is also useful for small corrections of the total temperature measurement.

Total Temperature Sensor (Terminal Descent). During terminal descent, the total temperature is below 350^{o}K. Therefore, radiation effects from the probe walls are small and no more than two radiation shields are required. The full-range output corresponds to temperatures from 100^{o}K to 350^{o}K. All other considerations are similar or identical to those described for the total temperature probe mounted in the aeroshell module.

Terminal Descent Phase Mass Spectrometer. The tradeoff study for selection of mass spectrometer instruments showed that two types should be considered for terminal descent measurements. One type employs a quadrupole analyzer, the other an electrostatic and magnetic sector for mass separation. Both instruments were considered in preliminary design of the entry science package. In a quadrupole mass spectrometer (Figure 6), the ionized molecules are accelerated into the analyzer and subjected to superimposed dc and RF electrostatic fields so that only ions with specific mass will traverse the analyzer rods and reach the detector. In the double-focusing mass analyzer, the electric sector reduces energy aberrations of the ions. Mass separation occurs because the radius of the ion trajectory in the magnetic sector depends on the ion momentum. If only one ion detector is applied, the potentials for ion acceleration and electric sector must be scanned. The techniques for sampling and calibration common to both types of instruments are described first.

Sample flow is conducted to the mass spectrometer inlet leak area by a short sampling tube directed into the flow. The sample transport lag and absorption or desorption at the walls demand minimum length for this component. A continuous flow is maintained by venting to a wake region with a lower pressure than at the inlet. A minute fraction of total flow through the sampling tube is induced into the analyzer past a leak. The location of the sampling tube inlet to avoid contamination from capsule bus effects and the position of the exit to ensure positive flow without sonic shocking will both be determined by wind tunnel testing. A leak consisting of a sapphire sphere pressed against a hole in a hardened steel plate[40] was selected for the preliminary design. Linear characteristics over a pressure range of 100:1 were reported for such a ball-leak consisting of many minute leaks caused by the sphere roughness.

The short operating time for analysis during terminal descent makes it possible to eliminate active pumping as a means for pulling a sample into the analyzer. Instead, an evacuated volume of around 2000 cc is connected to the analyzer for this purpose. All constituents are pumped equally. The vacuum is maintained by sealing until the experiment is activated during terminal descent. Some provisions to maintain the vacuum during space flight may be needed. Using the leak described above, the instrument operating pressure of 5×10^{-5} millibars will not be exceeded during operation.

Various approaches for calibration of the mass spectrometer were considered. Carbon monoxide outgassing from the mass spectrometer walls and atmospheric carbon dioxide can be used as reference for the atomic mass unit scale. This feature, and an electron source to recalibrate the electron multiplier, may be sufficient. However, for the preliminary design shown in the schematic (Fig. 5), a "start signal" from the science data subsystem initiates puncture of a small ampule of a known gas and introduces it into the sampling tube near and ahead of the inlet leak. The mass spectrometer will conduct one analysis of the calibration gas sample to provide a check of leak rate, sensitivity, and scale for mass numbers. About 4 seconds after the calibration measurement, a delay circuit triggers the opening of the mass spectrometer seal and atmospheric analysis begins. A sweep signal then synchronizes the start of the mass spectrometer sweep. Synchronism with the science data subsystem timing is provided by the pulse rate of the timing signal.

Compared with the other atmospheric sensors, the mass spectrometer requires a relatively high data rate. Therefore, the data requirements for three concepts will be briefly discussed. The least number of data bits is required when the mass spectrometer is set for only a limited number (say 5) discrete mass points. Another approach would be to scan the complete range of atomic mass units and sample the ion detector output about eight times for each one. It was felt that this approach would require an excessive number of data bits in proportion to the essential information acquired. The third approach, and the one selected for preliminary design, is the peak search mode. During the mass scan of the analyzer, a sensor would search for the peaks of the spectrum, giving a signal to digitize when a peak in analyzer current output is found. One approach is to measure only when a mass peak occurs and to identify the atomic mass units by sensing the scan voltage for the peak or to use the time interval between start of scan and peak measurement. For the preliminary design, a 7-bit word is provided for each mass number and it is assumed that the scan voltage increases by a constant amount per mass unit. In the data automation system, a buffer storage capability of 112 7-bit words was provided. This buffer storage is read out every 8 seconds during terminal descent. For a mass range of 10 to 60 atomic mass units, fifty-six 7-bit words are sufficient to digitize one mass spectrometer scan, and one ion gage pressure measurement of the analyzer pressure, and to conduct several engineering measurements.

Engineering measurements of the quadrupole mass spectrometer operation will be taken periodically after every two mass spectrometer analyses. They would consist of five samples of the dc sweep voltage, one measurement each of the supply voltage for the electron multiplier, two bias voltages, the electron emission current of the ionizer, and one measurement from the thermal vacuum gage that monitors the mass spectrometer pressure. One analysis sweep will require about 2 seconds and will obtain about 350 bits of science data. Depending on the atmosphere encountered, from one to several minutes of analysis will be possible.

Figure 5 shows the configuration of a double focusing mass spectrometer. The arrangements for calibration, composition sampling, pumping, and electronic control are similar to those of the quadrupole mass spectrometer system. The double focusing mass spectrometer scans the mass range by changing the potentials of the ion accelerator electrode and of the electric sector.

A quadrupole or a double focusing mass spectrometer can equally well be incorporated in the entry science package. No significant difficulties are foreseen in adapting the science data subsystem to the specific data requirements.

<u>Humidity Sensor (Terminal Descent)</u>. Figure 7 shows the basic construction, a block diagram, and typical instrumentation characteristics of the humidity sensor. The hygroscopic aluminum oxide changes its conductance as a function of absolute water vapor concentration. Its characteristics are nearly independent of ambient temperature and pressure. Because of the low expected humidity (about -100°C frost point), great care is required to ensure that the humidity content of the sampled atmosphere is not altered by contact with any part of the flight capsule; thus location of the humidity sensor must be established by aerodynamic tests. The temperature of the mechanical support for the hygrometer will be measured.

For checkout of the electronics, a reference impedance is temporarily connected in place of the sensing element. Various approaches are possible to measure the impedance (100 to 1000 kilohms) of the aluminum oxide element. Figure 7 indicates a Wien oscillator that converts the hygrometer impedance to a pulse repetition rate that may be between 30 and 200 pps. The pulse rate is converted to a proportional voltage.

Total Pressure Transducer (Terminal Descent). The construction, circuitry, and checkout of the total pressure transducer are identical to the absolute stagnation pressure transducer described previously (Figure 4). Figure 7 shows the construction of the transducer and the shielded pitot tube. With this pitot tube design, the pressure measurement is rather independent of lander attitude during terminal descent.

Television. The entry television consists of three replaceable assemblies:

1) Television camera unit, entry (25 degree field of view);

2) Television camera unit, terminal descent and landing (4 degree field of view);

3) TV electronics unit.

Each camera uses a 1 inch hybrid vidicon (electromagnetic deflection and electrostatic focus) operated in a 280 scanline mode using the full format area (0.44 x 0.44 in.). The cameras are similar except for the lenses and the lens covers (Figure 8).

The entry camera is mounted in the apex of the aeroshell (Figure 9) and takes pictures of the Martian surface through a quartz window in gradually improving resolution from the end of the heating phase of the entry trajectory to aeroshell separation. Initial resolution and coverage allows correlation of the frames with orbiter television frames. The terminal descent camera operates from aeroshell separation through landing, culminating in a resolution of one meter/optical line pair just before vernier firing. Better resolution is achieved during vernier rocket operation, provided the rocket plumes do not greatly degrade the images. Tests showed that the plume caused a negligible loss of resolution[96].

As indicated in Figure 8, each camera unit comprises lens cover, iris, shutter, control mechanisms, lens, vidicon, deflection yokes, preparation lamp, preamplifier, photometer, high-voltage power supply, and the focus voltage regulator.

The high-voltage power supply takes coarsely regulated power from the television electronics unit and generates various highly regulated dc levels by dc-dc conversion. The highest voltage required is 500 volts. The preparation lamp is used to erase the residual image; using the defocused electron beam, the photoconductor is charged to a uniform potential. The photometer output is used to control the iris setting through a servo and to provide a shutter-inhibit signal in case of excessive scene luminance (camera pointed at the sun).

The analog-to-digital converter samples the video output at 240 samples/line and converts the samples to 6-bit binary codes. The analog-to-digital conversion rate is controlled by the clock signal from the science data subsystem, ensuring full synchronization.

Subsystem Operation

Subsystem

The entry science subsystem consists of the instruments and the electronic equipment necessary to control and sequence the acquisition and formatting of science data. In a broad sense, the input to the entry science subsystem is the response of the instrument sensors to stimulus by the entry environment. Its output is a formatted digital bit stream of encoded science data.

Equipment. The entry science subsystem comprises the science instruments, instrument probes, science data subsystem, associated signal conditioning units, and engineering/status instruments. The location and installation of the hardware elements are shown in Figure 9. The equipment is mounted in three locations -- at the apex of the aeroshell for instruments that acquire data before staging; near the capsule bus center of gravity for the accelerometer triad, which acquires data throughout entry; and in an entry science package equipment module on the capsule bus for instruments that acquire data after staging. The signal conditioning electronics and science data subsystem units are also in this module. The equipment uses 28^{+4}_{-5} vdc and, after deorbit, thermal control is provided by electrical heaters. Table 2 lists the primary components of the entry science subsystem and gives their associated weights, dimensions, volume, and power consumption.

Functional Description. Figure 11 is a block diagram of the entry science subsystem and Figure 9 shows the equipment installation. The instruments and instrument probes are in two groupings based on general location -- on the aeroshell or on the capsule bus. The functional association of the instruments with the signal conditioning units and the data collection, storage, and multiplexing channels within the science data subsystem is shown.

Vibrating-diaphragm and stretched-diaphragm stagnation pressure sensors are at the apex of the aeroshell. The signal conditioning elements for the former are located in the aeroshell signal conditioner; those of the latter are self-contained. The instruments sample from a common probe mounted through the apex of the aeroshell (close to the quartz window). The entry phase mass spectrometer is adjacent to the quartz window, with its ion source through the aeroshell. All associated signal conditioning electronics and engineering sensors are packaged within the instrument. Both the entry television camera and total temperature probe are exposed for operation when the window cover is ejected at termination of the entry heat pulse. The camera is protected with an internal lens cover that is electromechanically removed for each exposure. All equipment is electrically connected to elements located in the capsule bus by a single cable assembly passing through an electrical disconnect.

The accelerometer triad is located on the capsule bus ahead of and near the cg. It consists of three force balance accelerometers on a common base, with their sensing axes mutually normal and parallel to the principal axes of the flight capsule. Servoamplifier and power conditioning circuit elements for these instruments are in the entry science package equipment module signal conditioning unit.

Humidity, total temperature, total pressure, and terminal phase mass spectrometer measurement samples are taken through individual fixed probes after aeroshell staging. These probes are mounted at the entry science package equipment module and extend to the side with openings pointing downward. The aluminum oxide humidity sensor is mounted on the probe and its associated electronics are in the signal conditioner. The total temperature probe also has its associated electronics in the signal conditioner. The stretched diaphragm pressure transducer contains its associated electronics. The terminal phase mass spectrometer also contains its associated electronics and engineering sensors and a calibration gas sample is also carried for this instrument. The instrument is pyrotechnically activated and calibrated. The narrow-angle television camera is in the entry science package equipment module for high-resolution imaging during terminal descent. It shares the television electronics unit with the wide-angle camera. The television electronics unit contains a separate and complete group of electronics for each camera, as well as signal conditioning circuitry for all television engineering measurements.

Sequence of Events

Figure 11 shows the entry science mission profile and the sequence of major events. The sequences are controlled by the science data subsystem sequencer-timer unit and are initiated by major event commands from the capsule bus sequencer-timer decoder. These include power turnon (30 minutes before entry), 800,000 ft altitude, 3,000 fps inertial velocity, aeroshell separation (15,000 ft altitude), 4,500 ft altitude, vernier shutdown, and power shutdown signals.

Based on receiving the above commands, the sequencer-timer unit sequences and times functions and events. Backup signals to critical sequencer-timer-issued signals are also initiated by the capsule bus sequencer-timer decoder.

Data Handling

The science and engineering data taken during entry into the Martian atmosphere are processed, formatted, sequenced, stored, and presented for transmission by the science data subsystem (see Figure 11, Functional Block Diagram of the Entry Science Subsystem).

The science data subsystem is located in the entry science package equipment module and consists basically of a data control unit and a data storage unit. It collects analog data samples from the science instruments, converts the samples to a 10-bit binary code, and multiplexes these data with buffered digital data from the mass spectrometers into a digital data stream that is serially written into the storage unit. The stored data are read out to the communication subsystem on a time-sharing basis with the TV digital data when the VHF links are transmitting to the spacecraft. The science data subsystem provides two redundant data output channels to the communication subsystem.

The analog-conditioned outputs of the science instruments (except TV and mass spectrometers) are paralleled with the science data subsystem input channels on individual wire pairs to the capsule bus telemetry encoders. The capsule bus communication link is used as a functional redundant route for transmitting analog entry science data.

The science data subsystem sequencer-timer initiates warmup power to the science subsystem prior to entry; initiates the data collection sequence on entry into the atmosphere at an 800,000 foot altitude; initiates the instrument calibration sequence; initiates power turnon to the UHF transmitter; sequences television image data with the other science data from the static storage unit; initiates changes in data format through the entry period; initiates the postentry calibration cycle; and initiates entry science power shutdown after capsule landing on the surface.

The above sequencer-timer functions are triggered by primary and secondary backup commands received from the capsule bus sequencer, timer-decoder unit, or the guidance and control computer. These primary and secondary commands are such flight capsule events as entry, 3,000 fps inertial velocity, aeroshell staging, vernier engine start and shutdown, and entry package shutdown.

Science data collection commences at the 800,000 ft altitude. Table 3 is a summary of the entry science data for three atmosphere models. Data collected at this time are represented by Format A, Table 4, and include atmospheric composition, stagnation pressure, and acceleration data. This data period lasts until the flight capsule decelerates in its ballistic entry to an inertial velocity of 3,000 fps.

Data collected in Format A are not transmitted in realtime but are stored in the science data subsystem static storage unit. The UHF transmitter is not turned on until the entry velocity is below 3,000 fps and the possible communication blackout period is past. Below the inertial velocity of 3,000 fps, the UHF transmitter is turned on and science data are relayed to the spacecraft.

The next entry data period commences after the entry velocity of 3,000 fps is reached and lasts until the aeroshell is staged. Data taken during this period are identified in Format B, Table 5 and in television data, Table 7. The science measurements taken during this period are the same as those taken during the previous period except that a television imaging sequence of the planet surface is also started.

The final entry data period, represented by Format C, Table 6, starts at aeroshell staging and lasts through the remaining portion of flight, which is called the terminal descent and landing phase. The entry instruments located on the aeroshell have separated and data are collected by terminal descent instruments located on the lander. The Table 6 format identifies the stored data taken during this period. In addition, surface imaging by the terminal descent and landing television camera is obtained throughout this period.

The science data subsystem, Figure 11, sequences the non-real-time stored science and engineering data with the real-time television image data. The output data rate of the subsystem to the VHF telemetry transmitter is 50,000 bps. At this data rate, the real-time television sequence requires 8.4 seconds of transmission time (420,000 bits of image data). The 100,000-bit static storage unit is read out and transmitted in 2 seconds. During the 2-second static storage readout, the television vidicon is erased, prepared for a new image, and a new image is taken. The sequence of 8.4-second television image transmission and the 2-second static storage readout is maintained throughout the entry data transmission period.

Redundancy of Measurements

Independent backup for every critical measurement was one of the system design objectives. Figure 12 indicates the backup to determine the various atmospheric parameters. The various events are easily correlated because the time of all measurements will be known.

Knowledge of capsule altitude and location are needed. The trajectory can be reconstructed from data supplied by the inertial guidance system. Capsule separation from the orbiter and the landing site serve as reference points. The accelerometer triad of the entry science package is a backup for part of the inertial guidance system. In addition, the altitude-marking radar measures altitude with a precision of ±40 feet below 800,000 feet. The terminal descent and landing radar determines range with an accuracy of ±4.5 percent or ±5 feet, whichever is larger. Inertial guidance and the terminal descent and landing radar also provide velocity measurements.

If the ballistic coefficient and velocity of the entry capsule are known, then atmospheric density can be determined from drag deceleration measured by the accelerometer triad (References 11 and 17). Atmospheric pressure is determined by the density column above the pressure point. Therefore, density integration versus altitude also yields the atmospheric pressure ($P_h = \int_h^\infty \rho g \, dh$). If the mean molecular weight or the composition is known, atmospheric temperature can be calculated ($T = \bar{M}P/[\rho R]$). At high velocities, stagnation pressure yields density quite accurately. The high-altitude mass spectrometer measures composition and partial number densities in the mass analyzer. These measurements can be correlated to ambient composition and density. Again, pressure and temperature can be calculated. The temperature calculation from the altitude rate of change of the ratio of any two constituents was described earlier.

From the total temperature (T_t) measurement below Mach 5, the composition or mean molecular weight ($\bar{M}$), and the specific heat ratio (γ), the ambient temperature (T_a) can be determined

$$T_a = \frac{2\,T_t}{2 + (\gamma - 1)\,M^2} \quad \text{where}$$

M is the Mach number.

After aeroshell deployment, the total temperature is little above ambient temperature and it is easy to determine ambient temperature rather accurately. This is also true for the total pressure. At Mach 0.4, the total pressure is only about 12 percent above ambient pressure.

The low-altitude mass spectrometer provides data about composition and the partial pressures. Thus, total ambient pressure also can be determined. The high-altitude mass spectrometer provides some backup for the low altitude composition measurements because considering the process of photodissociation and diffusive separation, the high-altitude data can be extrapolated to the lower atmospheric composition.

The sensing surface of the aluminum oxide hygrometer is directly exposed to the atmosphere and can therefore provide accurate measurements at very low humidities (below the -60°F frostpoint). Probably several sensing elements will be commutated to the instrument electronics. However, except for the absorption/desorption effects on the sampling tube surfaces, the low-altitude mass spectrometer can measure humidity with good sensitivity and accuracy and therefore provide some backup for the hygrometer.

The measurements of atmospheric pressure and temperature by the surface laboratory provide additional backup. If one of the atmospheric parameters -- density, pressure, temperature, or mean molecular weight -- is not sensed, the missing parameter can be calculated.

These backup measurements, combined with stringent standards of reliability, provide high confidence in mission success. Continued efforts of system studies and instrument development are needed to assure high reliability, best experiment approach, and optimum instrument performance.

ACKNOWLEDGMENT

This work was performed in part under Contract 952001 for the Jet Propulsion Laboratory, California Institute of Technology, as sponsored by the National Aeronautics and Space Administration under Contract NAS7-100.

REFERENCES

1. Performance and Design Requirements, 1973 Voyager Mission. SE002-BB001-1B21. Jet Propulsion Laboratory, January 31, 1967.

2. T. W. Neumann: Study of the Automated Biological Laboratory, Project Definition, Vol III, System Engineering Studies, Final Report. N67-16577. Martin Marietta Corporation, Denver Division, September 10, 1965.

3. F. S. Johnson: "Atmosphere of Mars." Science, December 10, 1965, p 1445-1448.

4. L. P. Kaplan, G. Munch, and H. Spinrad: Journal of Astrophysics, 139, 1, 1964.

5. W. E. Wagner: "Reentry Filtering Prediction and Smoothing." J. Spacecraft and Rockets, Vol 3, No. 9, September 1966.

6. S. C. Sommer, A. G. Boissevain, L. Yee, and R. C. Hadlund: The Structure of an Atmosphere from Onboard Measurements of Pressure, Temperature, and Acceleration. NASA TN D-3933 National Aeronautics and Space Administration, April 1967. Also S. C. Sommer and A. G. Boissevain: "Atmosphere Definition with a Free-Falling Probe." Astronautics and Aeronautics, February 1967.

7. R. F. Haines: A Review of the Expected Visual Environment of Mars and a Discussion of Some Questions Related to Visual, Photographic, and Radiometric Experiments. Ames Research Center, 1966.

8. L. G. Wolfert: Selection of Instruments for Measurement of Structure of the Martian Atmosphere. ED-22-6-102. Martin Marietta Corporation, Denver Division, June 1967.

9. L. G. Wolfert: Selection of Instruments for Measurement of the Composition of the Martian Atmosphere. ED-22-6-103. Martin Marietta Corporation, Denver Division, June 1967.

10. M. Kardos: Selection of Conceptual Designs for the Data Automation System, Voyager Entry Package Science Subsystem. ED-22-6-104. Martin Marietta Corporation, Denver Division, June 1967.

11. T. F. Swale: "Selection of a Conceptual Design for Entry Television Imaging Subsystem". ED-22-6-101. Martin Marietta Corporation, Denver Division, August 1967.

12. L. M. Jones, J. W. Peterson, E. J. Schaefer and H. F. Schulte: "Upper-Air Densities and Temperature from Eight IGY Rocket Flights by the Falling-Sphere Method". IGY Rocket Report Series Number 5, December 1, 1959.

13. K. S. W. Champion and A. C. Faire: Falling Sphere Measurements of Atmospheric Density, Temperature and Pressure up to 115 Km. AFCRL-64-554, July, 1964.

14. L. G. Jacchia: "Variations in the Earth's Upper Atmosphere as Revealed by Satellite Drag." Reviews of Modern Physics 35, 1963, p 973-991.

15. D. C. King-Hele and H. M. Rees: "The Decrease in Upper-Atmosphere Density between 1957 and 1963, as Revealed by Satelite Orbit." Royal Aircraft Establishment, Technical Note No. Space 32, 1963.

16. W. E. Wagner: Statistical Trajectory Estimation Program. ER 14075-I, Martin Marietta Corp., Baltimore Division, May 1966.

17. A. Seiff and D. E. Reese, Jr.: "Use of Entry Vehicle Responses to Define the Properties of the Mars Atmosphere." Advances in the Astronautical Sciences, Vol 19, AAS Symposium on Unmanned Exploration of the Solar System, Denver, Colorado, February 1965.

18. V. L. Peterson: A Technique for Determining Planetary Atmosphere Structure from Measured Accelerations of an Entry Vehicle. NASA TN D-2664, February, 1965.

19. V. L. Peterson: Analysis of the Errors Associated with the Determination of Planetary Atmosphere Structure from Measured Accelerations of an Entry Vehicle. NASA TR R-225. July, 1965.

20. J. H. deLeeuw and J. B. French: Operational Considerations for the Martian Atmospheric Entry Experiment. AEROCOL Report, Project 67-10, July, 1967.

21. S. H. Maslen: "Entry Science Measurements." Interdepartmental Communication, Research, Martin Marietta Corp., (RIAS), Denver, July 5, 1967.

22. D. J. Romeo: Analytical Study of Air Data Equations for a Hemispherical Pressure Probe in the Mach Number Range of 0 to 20. Cornell Aeronautical Laboratory Technical Report, September 1967.

23. K. S. Levinsky and H. Yoshehara: Rarefied Hypersonic Flow over a Sphere, Hypersonic Flow Research. (edited by F. R. Riddell) Academic Press, New York, N. Y., 1962, p 81-106.

24. J. L. Potter and A. B. Gailey: "Pressures in the Stagnation Region of Blunt Bodies in Rarefied Flow." AIAA Journal, Vol 2, N, 4, April 1964, p 743-745.

25. Final Report, Mars Probe/Lander Density-Sensing System. Giannini Controls Corporation for NASA-Langley Research Center, Contract NAS1-5341, February 1966.

26. C. A. Ziegler and B. Sellers: Radioisotope and Radiation Techniques for Terrestrial and Planetary Gas and Solid Measurements, Radio Isotopes for Aerospace, Part 1. Plenum Press, New York, N. Y. 1966, p 393-413.

27. P. V. Marrone: Rotational Temperature and Density Measurements in Underexpanded Jets and Shock Waves Using an Electron Beam Probe. UTIAS Report No. 113. April 1966.

28. D. E. Rothe: "Electron Beam Studies of the Diffusive Separation of Helium-Argon Mixtures." Phys. Fluids, 9, 1966, p 1643.

29. E. P. Muntz, and D. J. Marsden: Electron Excitation Applied to the Experimental Investigation of Rarefied Gas Flows. Vol II, Rarefied Gas Dynamics Third Symposium Academic Press, 1963, p 495. (edited by J. A. Laurmann)

30. V. I. Krassovsky: "Exploration of the Upper Atmosphere with the Help of the Third Soviet Sputnik." Proc. I.R.E., Vol 47, 1959, p 289-296.

31. R. E. Bourdeau: Ionospheric Results with Sounding Rockets and the Explorer VIII Satellite. Space Research II Proc. Int. Space Sci. Symp. Florence, 1961, North Holland Publishing Co., Amsterdam, 1961, p 554-573, (edited by H E. van deHulst.

32. N. W Spencer, L H. Brace, and G. R. Carignan: "Electron Temperature Evidence for Nonthermal Equilibrium in the Ionosphere." J. Geophys. Res., Vol 67, 1962, p 157-175.

33. R. A. Hanel, L. E. Richtmyer, R. A. Stampfl, and W. G. Stroud: Experiments from a Small Probe which Enters the Atmosphere of Mars. NASA TN D-1899.

34. J. O. Arnold, V. H. Reis, and H. T. Woodward: Theoretical and Experimental Studies of Equilibrium and Nonequilibrium Radiation to Bodies Entering Postulated Martian and Venusian Atmospheres at High Speeds. AIAA Paper No. 65-116.

35. H. T. Woodward: Predictions of Shock-Layer Radiation from Molecular Band System in Proposed Planetary Atmospheres. NASA TN D-3850. February 1967.

36. W. A. Menard, G. M. Thomas, and T. M. Helliwell: Experimental and Theoretical Study of Molecular, Continuum, and Line Radiation from Planetary Atmospheres. AIAA Paper No. 67-323.

37. E. E. Whiting: Determination of Mars Atmospheric Composition by Shock-Layer Radiometry during a Probe Experiment. AIAA Paper No. 67-293.

38. R. L. McKenzie: An Estimate of the Chemical Kinetics behind Normal Shock Waves in Mixtures of Carbon Dioxide and Nitrogen for Conditions Typical of Mars Entry. NASA TN D-3287. February 1966.

39. F. J. Hindelang: Coupled Vibration and Dissociation Relaxation behind Strong Shock Waves in Carbon Dioxide. NASA TR-R-253. February, 1967.

40. A Discussion of the Technology Base for a Mars Atmosphere Entry Experiment. The Aerodynamics Research Department, Cornell Aerodynamics Laboratory, Inc.

41. E. P. Muntz: Measurement of Rotational Temperature, Vibrational Temperature and Molecule Concentration in Nonradiating Flows of Low-Density Nitrogen. UTIA Report No. 71. University of Toronto, Institute for Aerospace Studies, 1962.

42. F. Robben and L. Talbot: Physical Fluids 9. 1966, p 644.

43. P. V. Marrone: Physical Fluids 10. 1967, p 521.

44. D. I. Sebacher: Proceedings of the Heat Transfer and Fluid Mechanics Institute. Stanford University Press, 1966.

45. S. L. Petrie: Proceedings of the Heat Transfer and Fluid Mechanics Institute. Stanford University Press, 1965.

46. D. E. Rothe: Physical Fluids 9, 1966, p 1943.

47. E. P. Muntz and D. J. Marsden: Rarefied Gas Dynamics. Academic Press, New York, N. Y., 1963. (edited by J. A. Laurmann)

48. A. G. Koval, V. T. Koppe, and Ya. M. Fogel: "CO, CO_2 and NO Emission Spectra Excited by 13 KeV Electronics." Soviet Astronomy 10, July-August 1966, p 165. Also A. G. Koval, V. T. Koppe, and Ya. M. Fogel: "Emission Spectra of Rarefied Molecular Gases Excited by Fast Electronics." Cosmic Research (Soviet) 4, 1966.

49. R. L. McKenzie and J. O. Arnold: Experimental and Theoretical Investigations of the Chemical Kinetics and Nonequilibrium CN Radiation behind Shock Waves in CO_2-N_2 Mixtures. AIAA Paper No. 67-322.

50. A. G. Boyer and E. D. Muntz: "Experimental Studies of Turbulence Characteristic in the Hypersonic Wave of a Sharp Slender Cone." Presented at the AGARD Meeting on Wakes, Denver, Colorado, May 1967.

51. J. G. G. Dionne, C. M. Sadowski, L. Tardif, and J. E. H. Vaneverschelde: "Mass Density Measurements in Hypersonic Wakes." Presented at AGARD Meeting on Wakes, Denver, Colorado, May 1967.

52. E. J. Schaefer: "Temperature and Composiion of the Lower Thermosphere Obtained from Mass Spectrometer Measurements." Presented at COSPAR, London, England, 1967. (To be published in Space Research VIII)

53. P. A. Redhead, J. P. Hobson, E. V. Kornelson: "Ultrahigh Vacuum." Advances in Electronics Physics, Vol 17, 1962.

54. L. J. Rigby: "Interactions of Nitrogen and Carbon Monoxide on Polycrystalline Tungsten." Canadian Journal of Physics, Vol 42, 1964, p 1256. Also, Can. J. Phys, Vol 43, 1965, p 1020.

55. E. J. Schaefer: Neutral Composition. University of Michigan Scientific Report 05627-3-S, Department of Aerospace Engineering, High Altitude Engineering Laboratory, February 1966.

56. E. J. Schaefer, M. H. Nichols: Upper Air Neutral Composition Measurements by Mass Spectrometer. University of Michigan Scientific Report 05627-2-S, High Altitude Engineering Laboratory, January 1964.

57. M. Nicolet: Physics of the Upper Atmosphere. Academic Press, New York and London, 1960, p 29-35. edited by J. A. Ratcliffe)

58. E. J. Schaefer and M. H. Nichols: "Neutral Composition Obtained from a Rocektborne Mass Spectrometer." Space Research, Vol 4, 1964, p 205-234.

59. E. J. Schaefer and M. H. Nichols: "Upper Air Neutral Composition Measurements by a Mass Spectrometer. Journal of Geophysics Research, Vol 69, No. 21, 1964, p 4649-4660.

60. R. J. Vidal, G. T. Skinner, and J. A. Bartz: "Speed-Ratio Measurements in Nonequilibrium Nozzle and Free-Jet Expansions." Rarefied Gas Dynamics, Academic Press, 1967. (edited by C. L. Brundin)

61. W. Gracey: Measurement of Static Pressure on Aircraft. Report 1364. National Advisory Committee for Aeronautics, 1958.

62. J. E. Ainsworth, D. F. Fox, and H. E. La Gow: Measurement of the Upper-Atmosphere Structure by Means of the Pitot-Static Tube. NASA Technical Note TN 670.

63. J. J. Horvath, R. W. Simmons, and L. H. Brace: Theory and Implementation of the Pitot-Static Technique for Upper-Atmospheric Measurements. Scientific Report No. NS-1. University of Michigan, March 1962.

64. W. Behrens: "Viscous Interaction Effects on a Static Pressure Probe at M-5." AIAA Journal, Vol 1, No. 12, December 1963, p 2864-2866.

65. D. J. Rigali and K. J. Touryan: Analysis of Pressure Measurements Taken at Altitudes between 20 and 90 Kilometers by Cone Cylinder Pitot-Static Probes. Sandia Report SC-RR-67-251. June 1967.

66. J. L. Potter, M. Kinslow, and D. E. Boylan: An Influence of the Orifice Cone-Measured Pressures in Rarefied Flow and Rarefied Gas Dynamics. Academic Press, New York, N. Y., 1966, p 151-174. (edited by J. H. DeLeeuw)

67. A. C. Combs, H. K. Weickmann, C. M. Mader, and A. Tebo: "Application of Infrared Radiometers to Meteorology." Journal of Applied Meteorology, April 1965, p 253-262.

68. Model 14-202 Free Air Thermometer. Product Data Bulletin, Barnes Engineering Company, February 11, 1966.

69. R. W. Cowne: Atmospheric Temperature Measurements from Aircraft. Preprint No. 19.1-4-64, 19th ISA Conference and Exhibit, October 12-15, 1964, New York, N.Y.

70. J. R. Mather, et al.: Developments in Meteorological Sensors and Measuring Techniques to 150,000 Feet, 1966. AD 653 622. C. W. Thornthwaite Associates, Centerton, New Jersey, June 1967.

71. A Survey for Naval Ordnance Laboratory of High Altitude Atmospheric Temperature Measurements, Final Report. AD 278 152. Wright Instruments, Inc., Vestal, New York, 1961.

72. T. G. Hames, W. M. Peake, B. C. Potts, and J. Shaw: Preliminary Analysis of Methods for Temperature Determination at Altitudes above 120,000 Feet. AD 242 206. Ohio State University, May 25, 1960.

73. H. N. Ballard: A Guide to Stratospheric Temperature and Wind Measurements. COSPAR Technique Manual Series, January 1967.

74. Total Temperature Sensors. Product Data Bulletin 7637, Rosemount Engineering Company, 1963.

75. D. Chleck and O. Cucchiara: "The Measurement of Oxygen in the Martian Atmosphere." International Journal of Applied Radiation and Isotopes, Vol 14, 1963, p 599-610.

76. Potential Planetary Atmosphere Sensors, Final Report. JPL Contract 950684, Parametrics, Incorporation, December 1964.

77. S. A. Hoenig and J. Abramowitz: Detection Techniques for Tenuous Planetary Atmospheres, Fifth Six-Month Report, July 1, 1965 - December 30 1965. NsG-458. Engineering Research Laboratories, University of Arizona.

78. AIM Keulemans: Gas Chromatography. Reinhold Publishing Company, New York, N. Y., 1964, Second Edition.

79. Gas Chromatographic Instrumentation for Analysis of the Martian Atmosphere, Final Report. N65-12617 CR59772. Melpar, Incorporated, September 25, 1962.

80. W. F. Wilhite: "Developments in Micro Gas Chromatography." Journal of Gas Chromatography, Febraury 1966.

81. A. O. Nier: A Study of the Feasibility of Employing a Magnetic Mass Spectrometer for the Analysis of the Martian Atmosphere. NASA N62-542. University of Minesota, December 20, 1962.

82. A Feasibility Study of the Mass Spectrometer Instrumentation for the Analysis of the Martian Atmosphere. NASA N66-11743 CR67959. Consolidated Systems Corporation, Space Science Department, September 1962.

83. Use of a Mass Spectrometer to Determine the Composition of the Undisturbed Martian Atmosphere from a Hypersonic Entry Vehicle. NASA CR71307 or N66-23779. General Electric Company, October 25, 1965.

84. C. A. Reber and L. G. Hall: A Double Focusing Magnetic Mass Spectrometer for Satellite Use. NASA TN D-3211. March 1966.

85. R. O. Woods and J. W. Ranftl: Instrumentation To Measure Mars Atmospheric Composition Using a Soft Landed Probe. Memorandum RM 4451 NASA. The Rand Corporation, April 1965.

86. Final Study Report, Phase 1, Development of a Two-Gas Atmosphere Sensor System. SDS Data Systems Corporation for NASA-Langley Research Center, Contract No. NAS1-5679, SDS Register No. 1-3006, March 1966.

87. Final Reports for JPL Contracts No. 950207 and No. 950685, Meteorology Research Inc.

88. Final Report for JPL Contract 950285 under Contract NAS7-100, Honeywell, Inc., November 30, 1962.

89. L. C. Paine and H. R. Farrah: "Design and Applications of High-Performance Dewpoint Hygrometers." Humidity and Moisture, Vol I. Reinhold Publishing Corporation, 1965, p 174-188.

90. Potential Planetary Atmosphere Sensors: The Cryptonate Oxygen Detector and the Aluminum Oxide Hygrometer. Parameterics, Inc., Waltham, Massachusetts, JPL Contract No. 950684 (N65-25246), December 31, 1964.

91. D. Chleck: "Aluminum Oxyde Hygrometer, Latoratory Performance and Flight Results." Journal of Applied Meteorology 5, December 1966, p 878-886.

92. D. Chleck and F. J. Brousaides: "A Partial Evaluation of the Performance of an Aluminum Oxide Humidity Element." Humidity and Moisture, Vol I. Reinhold Publishing Corporation, 1965, p 405-414.

93. Final Report, Lunar Facsimile Capsule Program. JPL Contract LC-950462 under Contract NAS7-100, 1963.

94. W. S. Beller: "Dielectric Camera Ready for Space Use." Missiles and Rockets, April 28, 1966, p 28.

95. L. R. Baker: The Development of a Sterilizable, Ruggedized Vidicon: Interim Results. JPL Space Program Summaries, 37-43 Vol IV, April 30, 1967, p 264-276.

96. J. D. Pernicka, R, Fearn, and H. K. Merril: Effect of Plumes on Optical Images and Systems. RA-614-67-1. Martin Marietta Corporation, Denver,Colorado, 1967.

97. H. E. Hinteregger: Space Astrophysics. McGraw-Hill Book Company, 1961, p 35-95. (edited by W. Liller)

98. R. A. Hanel, L. E. Richtmeyer, R. A. Stampfl, and W. G. Stroud: Experiments from a Small Probe which Enters the Atmosphere of Mars. NASA TN D-1899.

99. L. Talbot: "Theory of the Stagnation-Point Laugmnir Probe." The Physics of Fluids, March-April 1960, p 289-298.

100. W. C. Knudsen: "Evaluation and Demonstration of the Use of Retarding Potential Analyzers for Measuring Several Ionospheric Quantities." Journal of Geophysical Research, October 1, 1966, p 4669-4678.

101. R. E. Bourdeau, J. L. Donley, and Wipple, Jr.: Instrumentation of the Ionosphere Direct Measurements Satellite (Explorer VIII). NASA TN D-414. April 1962.

102. D. N. Vachon: The Density Structure of the Upper Atmosphere of Mars. R625D58-Class I. General Electric Company, Missile and Space Vehicle Department, May 1962.

103. G. Fjeldbo, W. C. Fjeldbo, R. VonEshelman: "Atmosphere of Mars: Mariner IV Models Compared." Science, Vol 152, 23 September 1966, p 1518-1523.

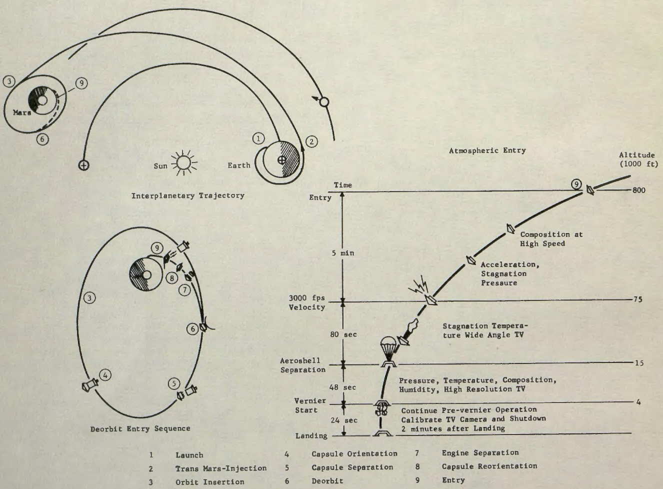

Figure 1 Reference Mission Profile

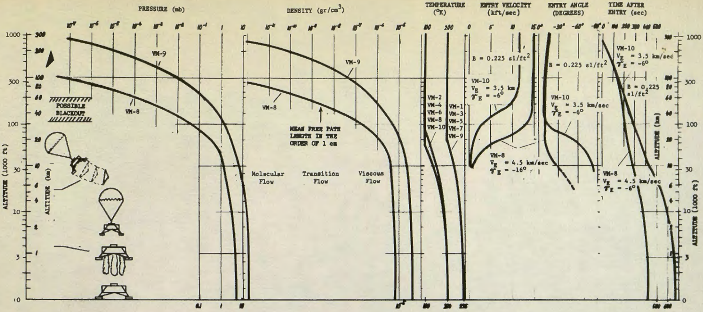

Constituents for Atmospheric Models

Model Atmosphere Composition (% by volume)	VM-1, 3, 5, 7, 9	VM-2, 8	VM-4	VM-6	VM-10
CO_2	20	100	68	29.4	9.5
N_2	80	0	0	32.2	70.5
A	0	0	32	38.4	20.0

Martian atmospheric water vapor content $(14 \pm 7) \times 10^{-4}$ g/cm^2-column [4].
Other possible trace constituents: O_2, N_2O, O_3, N_2O, CH_4, C_2H_6, NH_3.

Above 60 km altitude photodissociation and constituents such as O_1, N_2, CO, CO_2 and A are anticipated [103].

Electron density of 10^5 cm^{-3} at 120 km and electron scale heights of 25 to 29 km were reported.

Ions of O_1, O_2 and CO_2 were suggested [4].

Figure 2 Range of Some Parameters of Martian Atmosphere and Entry Flight

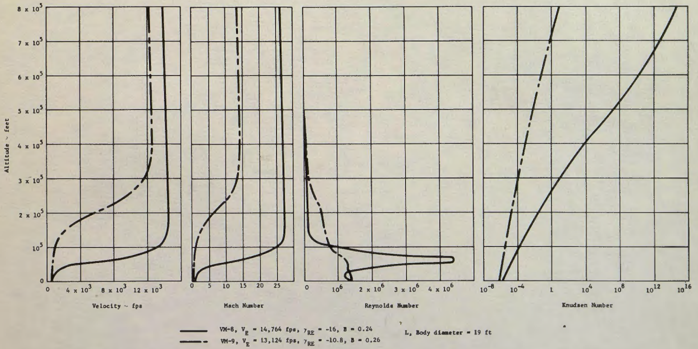

Figure 3 Martian Entry Flow Regimes

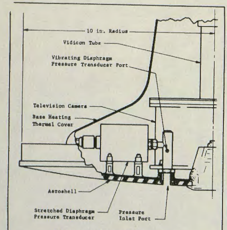

Installation of Pressure Transducers

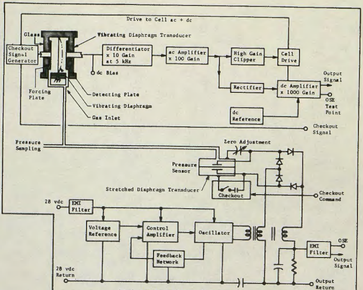

Block Diagram of Pressure Transducers

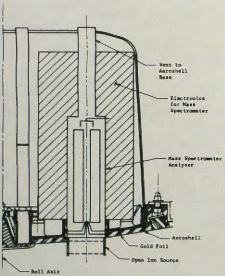

Cross Section of Installed Open Ion Source Mass Spectrometer

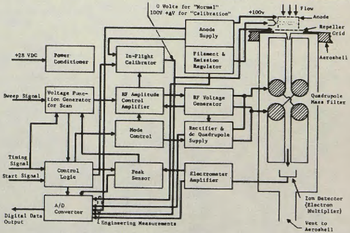

A Functional Schematic for Open Ion Source Mass Spectrometer

Characteristics of Open Ion Source Mass Spectrometer

Weight, total: 8 lb
Power: 6 w
Size: 11 x 3 in. dia
Mass Range: 1 to 50 AMU
Scan Time: 2 sec or more
Resolution: 50

Mode of Operation:

Peak mode and staircase mode alternately every fifth scan grid voltage is swept also to distinguish between incoming and reflected molecules.

Status:

Development of specific instrument needed.

Characteristics of Stretched Diaphragm Transducer Vibrating Diaphragm Transducer

	Stretched	Vibrating
Weight Sensor	10 oz	2 oz
Weight Electronics		3 oz
Power	+28 vdc, 1.4 w	+28 vdc, 1.5 w
Size Sensor	2.5x2-in. dia	0.6x0.8-in dia
Size Electronics		3 cu in.
Absolute Pressure Range	0 to 50 mb	0.0001 to 100 mb
Temperature Range Operating Sensors	-16°C to 80°C	-50°C to 155°C
Temperature Range Operating Electronics		4°C to 35°C desired.
Temperature Range Nonoperating Sensor	-54°C to 93°C	-50°C to 135°C
Temperature Range Nonoperating Electronics		-54°C to 33°C
Response Time	0.025 sec	< 0.025 sec
Data Requirement	10 bits/sample	10 bits/sample
Status	Developed, some modifications needed.	Sensor developed, electronics in redesign.

Figure 4 High Altitude Stagnation Pressure and Composition Measurements

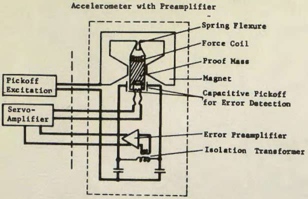

Single-Axis Accelerometer with Servo Loop

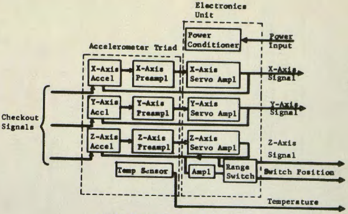

Block Diagram of Triaxial Accelerometer System

	Accelerometer Triad	Associated Electronics
Weight	20 oz	16 oz
Power		
Size	2.5x2.5x1.75 in. dia	9 cub in.
Acceleration Range	0 to 25 g and ± 0.5g	
Accuracy	Better than ± 0.001 g	
Temperature Range	-55°C to +80°C	-55°C to +80°C
Data Rate	30 bits/sample, 4 samples/sec	
Status	Basically developed; sterilizable unit can be available by early 1969	

Characteristics of Accelerometer Triad and Associated Electronics

Characteristics of Total Temperature Probes	Total Temperature Probe - Entry	Total Temperature Probe - Descent
Weight of Probe:	4 oz.	7 oz.
Weight of Electronics:	8 oz.	8 oz.
Power Total:	+28 vdc, 1 w	+28 vdc, 1 w
Size of Probe:	12 x 1 in. dia.	10 x 1 in. dia
Volume of Electronics:	5 cu in.	5 cu in.
Data Rate:	10 bits/sample	10 bits/sample
Sensor Range:	100°K to 1000°K	100°K to 350°K
Status:	Modification Needed	Similar probes in use New development needed

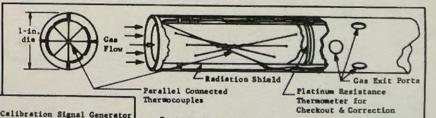

Basic Design for Total Temperature Sensor-Descent

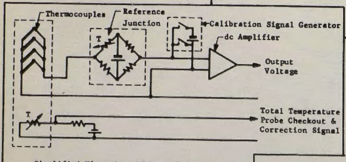

Simplified Electrical Diagram for Both Probes

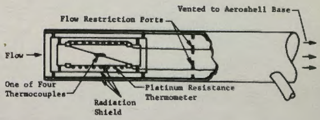

A Total Temperature Sensor for High Mach Numbers-Entry

Figure 5 Acceleration and Total Temperature Measurements

Characteristics of:	Quadrupole Mass Spectrometer	Double Focusing Mass Spectrometer
Weight Total:	8 lb	7 lb
Power:	10 w	7 w
Size:	8.6 x 14 x 2.8 in. plus gas sampling	13 x 8.6 x 27 in. plus gas sampling
Mass Range:	m/e 10 to m/e 60	m/e 10 to about m/e 80
Scan Time:	2 sec or more	About 2 sec
Resolution:	M/△ M - 50 at 30 amu	M/△ M = 150 at 100 amu
Dynamic Range:	10^4 (log. ampl.)	10^5 (dig. voltmeter)
Accuracy Approximately:	10% on 1% constituents or better 5% on 80% constituents or better	6% on 1% constituents 3% on 80% constituents
Data Output Assumed:	50 - 7 bit words for mass scan 6 - 7 bit words for eng. meas.	About 400 bits per scan About 5 - 7 words for eng. meas.

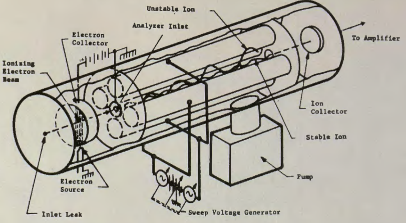

Basic Configuration of Quadrupole Mass Spectrometer

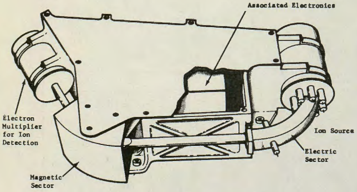

Configuration of a Double Focusing Mass Spectrometer Package

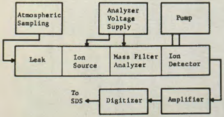

Basic Block Diagram of a Mass Spectrometer

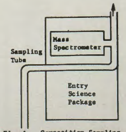

Composition Sampling

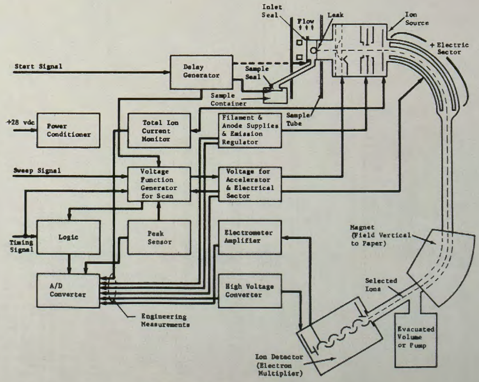

A Functional Schematic for Double Focusing Mass Spectrometer

Figure 6 Low Altitude Composition Measurement

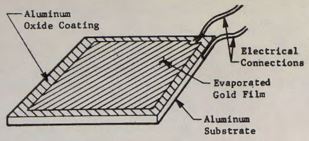

Construction of Aluminum Oxide Sensor

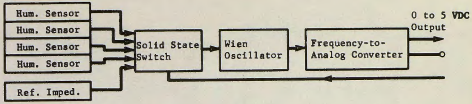

Block Diagram for Hygrometer Instrument

<u>Hygrometer Characteristics</u>

Weight of probe with sensor: About 3 oz
Weight of associated electronics: 5 oz
Power: 0.5 w
Size of Probe: About 10 in. long
Size of sensing element: 0.2x0.6x0.003 in. is typical
Volume of electronics: 2 cu in.
Range of sensor dew/frost-point temp: -150°C to +10°C
Data rate: 10 bits/sample
Time constant: About 1 sec claimed for 63% change
Status: Tests did not rule out use

<u>Characteristics of Pressure Transducer</u>

Weight: 10 oz
Power: +28 vdc; 0.05 amp; 1.4w
Size: 2.5x2 in. dia
Absolute Pressure Range: 0 to 40 mb
Time Constant: <0.025 sec
Data rate, each: 10 bits/sample
Status: Developed, some modification needed

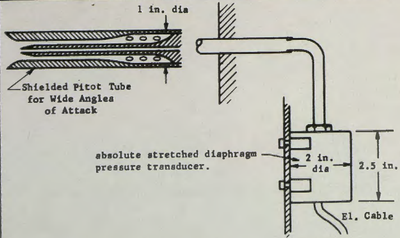

Installation of Total Pressure Probe & Transducer

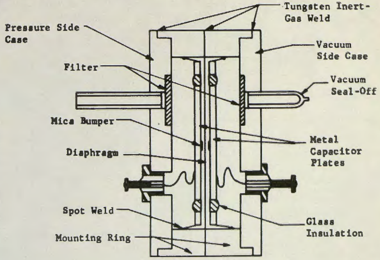

Construction of Pressure Transducer with
Stretched Diaphragm & Capacitive Pickoff

Figure 7 Low Altitude Humidity and Total Pressure Measurement

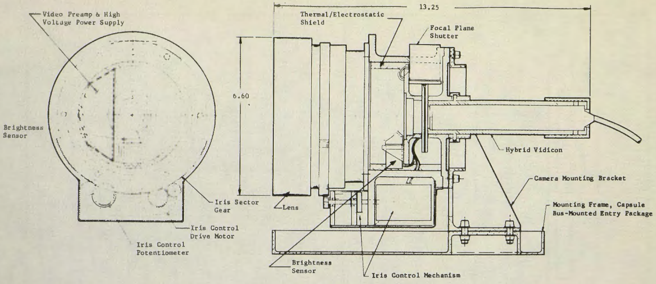

TV Camera Unit-Descent

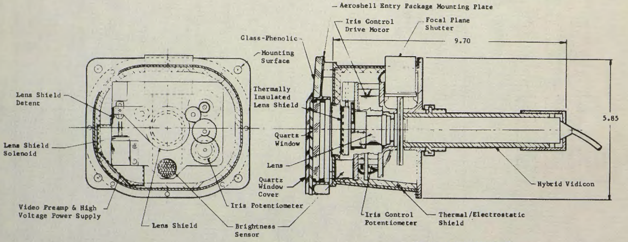

TV Camera Unit-Aeroshell

Television Equipment Performance Parameters

TV Camera Unit	Aperture Range	Settings at 360 ft-Lamberts Avg. Brightness	
		Aperture	Exposure Time (ms)
Entry	f/0.84 - f/4*	f/0.84	2
TDL	f/1.0 - f/4*	f/1.0	3

*At avg brightness of 6000 ft-lamberts.

1. Minimum detectable brightness = 10 ft-lamberts
2. Distinguishable levels = 12 grey shades ($\sqrt{2}$ steps)
3. Six-bit digitation of linearly amplified vidicon output
4. Signal-noise ratio (at input to AD converters) = 47 db for highlight signal, 12 db for low light signal
5. 200 television lines at limiting resolution
   280 scan lines — 240 digital samples/line
   6 bits per digital sample — 403,200 bits per picture

Photo No.	Area	Best Resolution (ft)
1	63,046 sq mi	436
2	9,288 sq mi	338
3	208.6 sq mi	228
4	70.24 sq mi	200
5	25.73 sq mi	152
6	10.51 sq mi	112
7	4.50 sq mi	82
8	1.48 sq mi	60
9	1,680,406 sq ft	12.6
10	1,047,550 sq ft	10.2
11	647,220 sq ft	8.04
12	348,690 sq ft	5.9
13	142,884 sq ft	3.8
14	82,656 sq ft	2.9
15	10,816 sq ft	1.04
16	134 sq ft	0.1

Figure 8 Surface Imaging

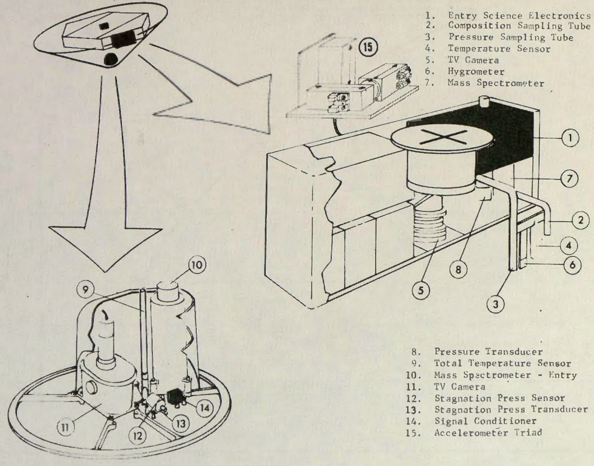

Figure 9 Equipment Installation

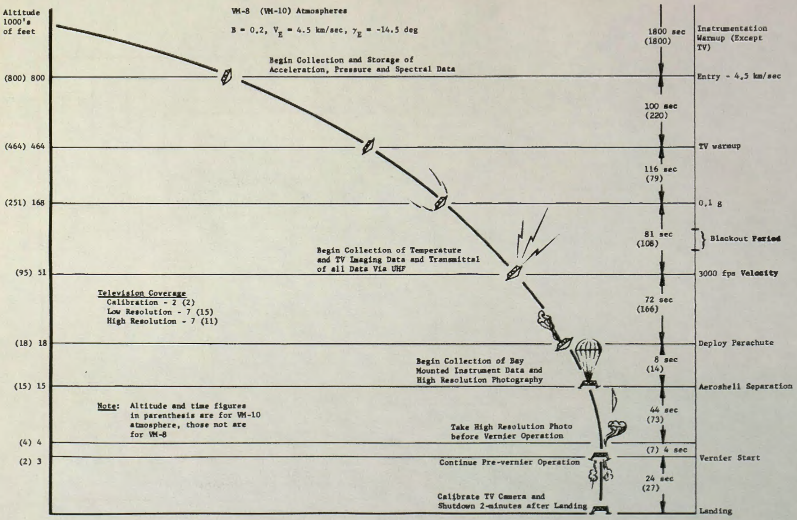

Figure 10 Entry Science Mission Profile and Sequence of Events

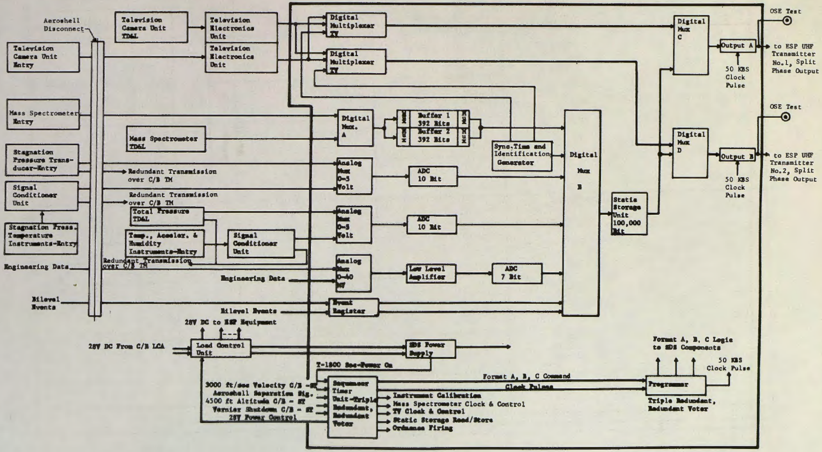

Figure 11 Functional Block Diagram of the Entry Science Subsystem

Entry	INSTRUMENTS	MEASUREMENT	STRUCTURE INFORMATION ρ	P	T	COMPOSITION
800,000 ft	Accelerometer Triad	Drag	X	(X)		
	Pressure Gage	Stagnation Pressure	X	(X)		
	Mass Spectrometer	Number Density of Constituents	X	(X)	(X)	X
Aeroshell Staging	Temperature Sensor	Total Temp below Mach 5			X	
15,000 ft 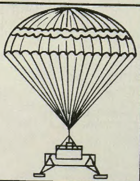	Pressure Gage	Ambient Pressure		X		
	Temperature Sensor	Total Temp			X	
	Mass Spectrometer	Relative Number Density of Constituents		X		X
Vernier Start	Humidity Sensor	Dew Point				X
4,000 ft 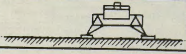	Continue Pre-Vernier Operation					
Surface	Surface Laboratory Measurements			X	X	X

Note: Knowledge of Trajectory vs Time is assumed
(X) Means not measured directly

Fig. 12 Backup of Entry Science Measurements

Table 1 Alternate Concepts for Surface Imaging and Measurement of Atmospheric Structure and Composition

COLUMN NO.	PRIMARY MEASUREMENT OBJECTIVES AND MEASUREMENT REGION	MEASUREMENT TECHNIQUES	MOUNTING REQUIREMENTS	PREVIOUS USE OF TECHNIQUE	EVALUATION OF PRELIMINARY DESIGN
1	Density From entry to parachute deployment	Accelerometer triad on roll axis near cg (ambient density from drag acceleration) $\rho_\infty = \left(\frac{m}{C_D A}\right) \frac{2}{U_\infty^2} a$ a = acceleration $\frac{m}{C_D A}$ = ballistic coeff.	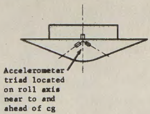	Drag of a falling sphere for high-altitude density (12, 13) Drag of satellites for high-altitude density (14, 15) Trajectory reconstruction for PRIME lifting reentry vehicle (5, 16) Atmosphere structure from onboard measurements on a planetary entry configuration (7) Studied extensively for Mars density profile from an entry vehicle (17, 18, 19)	<u>Selected</u> A well-established technique in atmospheric research on Earth Analytically studied in detail for research in planetary atmospheres Experimental verification for Voyager application through the PRIME & PEPP programs
2	Density Free-molecular through continuum flow	Stagnation pressure gage ambient density from $P_s \sim \rho_\infty U_\infty^2$ P_s - stagnation pressure ρ_∞ - ambient density U_∞^2 - free-stream velocity	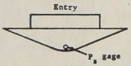	Reliable & proven technique for supersonic & subsonic measurements on aerodynamic bodies (6, 20, 21)	<u>Selected</u> Provides a reliable measurement of ambient density physically redundant to density obtained from drag Mounting requirements are simple
3	Density Throughout the entry & terminal descent & landing phases	γ-ray back scatter Number of backscattered γ-rays is a function of ambient gas density	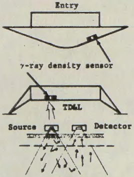	A conceptual design has been completed. Development of an engineering prototype is in progress. The technique could provide continuous direct measurement of atmosphere density from entry altitudes to the planet surface (25)	<u>Not Selected</u> Untried in atmospheric research at this time
4	Density Above 7×10^{-5} gr/cc	β-ray forward scatter Number of deflected β-rays is a function of ambient gas density	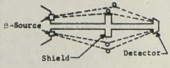	High altitude soundings (26)	<u>Not Selected</u> In experimental stage
5	Density Ground to 2.5×10^{-9} gr/cc	X-ray scatter gauge Compton scattering and/or photo electric effects caused by X-rays are utilized for measurement	Similar to gamma ray densitometer	High altitude soundings (26)	<u>Not Selected</u> In experimental stage

Table 1 (cont)

COLUMN NO.	PRIMARY MEASUREMENT OBJECTIVES AND MEASUREMENT REGION	MEASUREMENT TECHNIQUES	MOUNTING REQUIREMENTS	PREVIOUS USE OF TECHNIQUE	EVALUATION OF PRELIMINARY DESIGN
6	Density 2.5×10^{-9} to 5.5×10^{-13} gr/cc	Brems Strahlung Gauge An electron beam generates brems strahlung X-rays in gas. Part of these X-ray photons traverse collimator and reach X-ray detectors	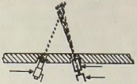	High altitude soundings (26)	Not Selected In experimental stage
7	Density Neutral Composition All altitudes	Electron-beam induced luminosity (Ambient density from luminous intensity) (Species partial densities from luminous spectra)	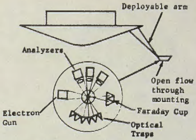	Low density wind tunnels for local density, temperature, & relative composition of Ar-He mixtures (27, 28) Rocket experiment in preparation at University of Toronto Institute for Aerospace Studies for obtaining atmosphere temperature & partial density of nitrogen at Earth altitudes of 70 to 180 km Considered for use with gases expected to be encountered on Mars (29)	Not Selected Untried in atmospheric research at this time Weight & complexity of deployable instrument arms not considered compatible with Voyager 1973 design constraints
8	Ion and/or electron density ion composition and electron temperature Throughout entry & terminal descent	Langmuir probe or modified probes with grids. Particle kinetic energy is measured with "potential hill" due to charged grid, current represents density. Ion kin. energy proportional to molecular weight.	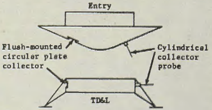	Widely used technique for atmospheric research from sounding rockets & satellites (30-32, 100,101)	Not Selected Information from charged-particle measurements not closely associated with entry science objectives for Voyager 1973 Measurements do not provide strong redundant information for structure determinations
9	Composition Applicable for densities above 10^{-12} gr/cc	Absorption Spectrometer Absorption of sunrays in selected IR and UV bands is measured. Selected spectrum bands are characteristic for specific constituents	Mounted in back with wide view angle to avoid shadows 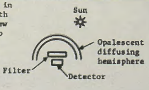	High altitude soundings (97, 98)	Not Selected Specific development needed
10	Composition Continuum flow during maximum aerodynamic heating of aeroshell	Emission Spectroscopy The light spectrum emitted from the hot gas indicates composition	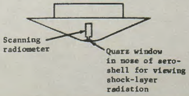	Much theoretical & experimental work in spectroscopic study of shock-layer radiation from planetary atmospheres has been done. Most of this work applies for stagnation temperatures near 5000°K (34-40)	Not Selected For Voyager 1973 stagnation temperatures of 2000 to 3000°K are more likely & radiation will be mostly in IR. Compsition information from expected radiation bands in this region is marginal in terms of 1973 entry science objectives

Table 1 (cont)

COLUMN NO.	PRIMARY MEASUREMENT OBJECTIVES AND MEASUREMENT REGION	MEASUREMENT TECHNIQUES	MOUNTING REQUIREMENTS	PREVIOUS USE OF TECHNIQUE	EVALUATION OF PRELIMINARY DESIGN
11	Density, composition Free molecular flow regimes at high altitudes	Mass spectrometer in cavity. Uses density enhancement in cavity due to high velocity (4 km/sec). In MS particles are ionized and separated by magnetic and/or electrostatic fields	 MS mounted in cavity connected to stagnation point	No known previous use. Concept considered because of density enhancement in the stagnation cavity. This can be as high as 40 & can raise by 20 km the altitude at which stable species may be detected (20)	Not Selected Untried in atmospheric research at this time Adsorption, desorption, & replacement reactions at cavity walls prevent unambiguous interpretation of results. Reactive species cannot be detected
12	Density, neutral or Ion composition Entry down to ambient pressures near 5×10^{-5} torr (See Fig. 1 of Ref 20)	Fly through mass spectrometer Molecular beam is defined out of free stream gas	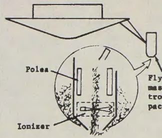	No known previous use. Concept considered because the flow-through device defines a molecular beam out of the free stream gas & uses vehicle motion to produce high vacuum around the beam. Range of unambiguous results obtained in free molecular flow may thus be extended downward approximately 30 km (20)	Not Selected Untried in atmospheric research at this time Weight & complexity of deployable instrument arms not considered compatible with Voyager 1973 constraints
13	Density, composition Free molecular flow regimes at high altitudes	Open ion source with repeller grid Open ion source minimizes surface interaction, repeller grid is used periodically for calibration to provide potential hill to exclude all particles except those with free-stream relative potential energy	 Special grid in ion source provides small retarding potential to exclude all particles except those with free-stream relative potential energy. Used periodically for calibration MS with repeller grid on aeroshell with open ion source projecting	Extensive background from Earth atmospheric research in use of mass spectrometer with open ion source (52, 55-59) Techniques applicable at Voyager 1973 entry velocities & using open forward-facing ion sources are being evaluated aboard present & planned satellite flights	Selected A strong experience base exists for implementing this technique Use of the retarding potential offers possibility for inflight and on-site calibration of the ion source Direct measurement of atmosphere composition at high altitude is considered a requirement for the mission
14	$\frac{RT}{m}$ Ratio Free-molecular flow regimes based on ambient mean free paths greater than 7 times the probe dimension	Molecular speed ratio probe $\frac{RT}{m}$ Ratio (R - universal gas constant T - Ambient temperature m - mean molecular weight) q_{st} = stagnation-point heat transfer q_{fp} = flat-plate heat transfer $\frac{q_{fp}}{q_{st}} \sim \sqrt{\frac{RT}{m}}$	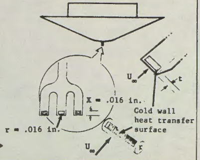	Evaluated for experimental instrumentation in non-equilibrium expansion processes research (60) Concept considered because of promising results from initial evaluation. The experimental quantity RT/m gives ambient T directly if m is known by mass spectrometer. Also, ambient pressure is given directly if knowledge of ambient density is obtained from drag measurements	Not Selected Untried in atmospheric research at this time Special requirements include cooling of heat transfer surfaces, maintaining surfaces so that accommodation coefficients are known, & projection of a probe from the vehicle. These requirements were not considered compatible with Voyager 1973 design constraints

Table 1 (cont)

COLUMN NO.	PRIMARY MEASUREMENT OBJECTIVES AND MEASUREMENT REGION	MEASUREMENT TECHNIQUES	MOUNTING REQUIREMENTS	PREVIOUS USE OF TECHNIQUE	EVALUATION OF PRELIMINARY DESIGN
15	Pressure Supersonic flow in the transition & continuum flow regimes	Multiple pressure probe Static pressure P_∞ is determined from two or more pressure measurements $P_\infty = P_2 \left[\frac{C_{P1} - C_{P2}\, P_1/P_2}{C_{P1} - C_{P2}}\right]$ C_{P1} and C_{P2} are calibration coefficients; P_1, P_2 are pressures	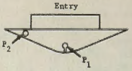	Technique has been used on PEPP Program below M2 (6)	Not Selected This technique requires investigations before it can be recommended
16	Pressure Supersonic and subsonic flow in the transition & continuum flow regimes	Side-port pressure probe Dynamic effects on sideport pressure are relatively small, therefore this pressure is close to ambient pressure	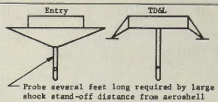	Technique of using probes in atmospheric research at high and low Mach numbers has been developed (61-63)	Not Selected Direct measurement of ambient pressure not significant enough in 1973 to justify added weight & complexity of the long static probe
17	Pressure During terminal descent	Total Pressure (P_t) Total pressure is the sum of ambient pressure and the pressure effect due to the flow dynamics of gas particles $P_t = 1/2\, \rho_\infty V_\infty^2 C_P + P_\infty$	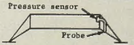 Probe sampling is insensitive to angle of attack & will provide pressures to sensor within a few percent of ambient	Techniques are well developed for the low velocities occurring during terminal descent (62, 63, 65)	Selected Direct measurement of low-altitude and surface pressure is considered a requirement for the mission
18	Temperature During entry and terminal descent	Radiation thermometer Narrow band IR emission intensity of gas is measure of gas temperature $E = K\left(T_1^{\,4} - T_2^{\,4}\right)$	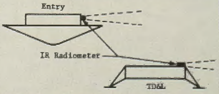	Used for gas temperature measurement from airplanes and for remote temperature sensing (67-69)	Not Selected Aerodynamically heated gas interfers, relatively heavy and complex instrumentation needed
19	Temperature During terminal descent	Vortex thermometer Adiabatic cooling near center of an air vortex compensates aerodynamic temperature rise	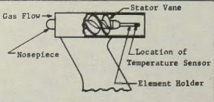 Deloyment as shown in column below	Used in some experimental aircraft applications. Sensitive to angle of attack (69)	Not Selected Sensitive to angle of attack and it is not possible to design a sensor for a wide range of flight conditions
20	Temperature During terminal descent	Immersion temperature sensor Conductive heat transfer from gas to sensing element	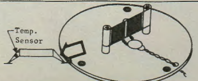	Used extensively on subsonic (M < 0.5) meteorological drop sondes (70-73)	Not Selected Directly exposed and less reliable, rather sensitive to flow conditions

Table 1 (cont)

COLUMN NO.	PRIMARY MEASUREMENT OBJECTIVES AND MEASUREMENT REGION	MEASUREMENT TECHNIQUES	MOUNTING REQUIREMENTS	PREVIOUS USE OF TECHNIQUE	EVALUATION OF PRELIMINARY DESIGN
21	Temperature At velocities below Mach 5	Total temperature sensor Total temperature of gas (T_o) is achieved when the gas is brought to rest (or nearly so) without removal of any heat $T_o = T_\infty \left[1 + (\gamma - 1) M^2/2\right]$	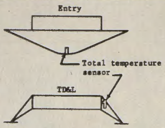	A broad background in use of atmosphere temperature sensors exists in the fields of aerospace & meteorological instrumentation (6, 8, 69, 74)	<u>Selected</u> Direct sensing of atmosphere temperature considered a required measurement for entry science in the Voyager 1973 mission Mounting requirements are simple
22	Composition During terminal descent	Kryptonate detectors Radioactive kryptonate is imbedded in material which is eroded by specific gas. Loss of radioactivity is sensed	Mounting requirements similar to gas chromatograph 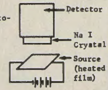	Technique in experimental stage (75-77)	<u>Not Selected</u> No extensive testing known
23	Composition During terminal descent	Gas chromatograph Gas is flushed through column(s) containing absorptive material or molecular sieves. Flush through period indicates composition	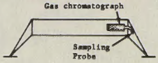	A micro gas chromotograph column has been developed for analysis of Martian atmosphere during entry descent (80) All other references to work in gas chromatography instrumentation for space application were found to be concerned with long-time use on planetary & lunar surfaces (9, 78, 79)	<u>Not Selected</u> Untried in atmospheric research at this time
24	Composition During terminal descent	Mass spectrometer with inlet leak Leak and pump reduce pressure. Then gas is inoized by electron beam and mass separation is achieved by magnetic and/or electrostatic fields. Concentration and composition (amu) are measured	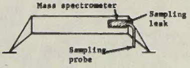	Extensive background in development & use of flight worthy instruments aboard satellites & sounding rockets Background also exists in development of sampling leaks for these instruments (9, 39, 81-86)	<u>Selected</u> Direct measurement of a atmosphere composition at low altitudes in considered a requirement for the mission
25	Humidity During terminal descent	Dewpoint hygrometer A small surface is cooled until dew/frost layer begins to form		Used for atmospheric measurements with airplanes, balloons and rockets (88, 89)	<u>Not Selected</u> It is difficult to cool sensing element below -60°C. Long response times at low humidity
26	Humidity During terminal descent	Phosphor pentoxide electrolytic hygrometer Based on electrolysis of water vapor absorbed by sensor	Mounting similar to that of dew point hygrometer	Used for measurements from balloons and airplanes (87)	<u>Not Selected</u> Compatability with sterilization and spaceflight environment could not yet be demonstrated

Table 1 (concl)

COLUMN NO.	PRIMARY MEASUREMENT OBJECTIVES AND MEASUREMENT REGION	MEASUREMENT TECHNIQUES	MOUNTING REQUIREMENTS	PREVIOUS USE OF TECHNIQUE	EVALUATION OF PRELIMINARY DESIGN
27	Humidity During terminal descent	Aluminum oxide hygrometer The electrical conductance changes due to water absorbed in the pores of the aluminum oxide	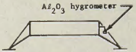 Mounted in stream of gas that has not contacted other structure	Aluminum oxide sensors have been used on balloon & rocket sondes for atmospheric research. Development work to demonstrate feasibility of the technique for humidity measurements in planetary atmospheres has been conducted (90-92)	Selected Promising technique based on use for atmospheric research in Earth atmosphere Instrument is simple & light & requirements are compatible with design constraints Measurement of atmosphere humidity content considered a requirement for the mission
28	Surface imaging During entry and terminal descent	Facsimile camera Single light detector with optical scan of image elements	The mounting requirements for all alternates for surface imaging are very similar 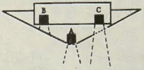 Three promissing approaches for mounting 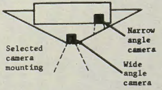 Rigidly mounted conventional vidicon cameras with retractive optics for a wide and a narrow field of view were selected	A facsimile camera for severe impacts has been developed and such a camera was used on Luna 9 and Luna 13 (93)	Not Selected Exposure time is too long
29	Surface imaging During entry and terminal descent	Photography with electro-optical scan of photograph		Lunar orbiters	Not Selected High resolution, but data cannot be transmitted before landing because of photograph development time. Complex instrument mechanism, high data rate per picture
30	Surface imaging During entry and terminal descent	Dielectric tape, drum or disc camera Image is stored on tape in dielectric form		A dielectric camera has been developed and qualified to Nimbus test level (94)	Not Selected This camera is heavy, not sterilizable, has relatively long exposure times and requires about 25 watts
31	Surface imaging During entry and terminal descent	Vidicon camera Image is recorded in form of electrostatic charges and scanned with electron beam		Many vidicon cameras have been applied in space projects such as: Nimbus, Tiros, Ranger, OAO (95)	Selected Vidicon camera is sterilizable, has best development status and good performance. Requirements for weight and power are relatively small.

Table 2 Weight, Volume and Power for the Entry Science Subsystem

Component / Parameter	Weight (lb)	Dimensions (in.)	Volume (cu in.)	Power (w)
Science Data Subsystem Control Unit	9.0		945.0	14.0
Science Data Subsystem Storage Unit	5.0		294.0 (Part of SDS control unit volume)	3.0
Signal Conditioner Unit	1.5	3 x 3 x 2	18.0	11.5
Television Electronics Unit	13.0	10 x 10 x 5	500.0	15.0
Television Camera Unit, TDL	11.7	13 x 7 x 7	637.0	2.5
Television Camera Unit, Entry	5.8	10 x 6 x 6	360.0	2.5
Mass Spectrometer, TDL	8.0	14 x 8.6 x 2.8	340.0	14.0
Accelerometer Triad	1.2	2.5 x 2.5 x 1.75	11.0	5.0
Total Pressure Transducer	0.6	2.5 x 2 dia	8.0	1.4
Humidity Sensor	0.2	10 x 1 x 0.1	1.0	*
Total Temperature Sensor	0.4	10 x 1 dia	8.0	*
Aeroshell Signal Conditioner Unit	1.0	3 x 2 x 2	12.0	2.9
Aeroshell Total Temperature Sensor	0.1	4 x 0.75 dia	3.0	*
Stagnation Pressure Transducer	0.6	2.5 x 2 dia	8.0	1.4
Stagnation Pressure Sensor	0.1	0.65 x 0.8 dia	0.4	*
Mass Spectrometer, Entry	3.0	10 x 5 dia	200.0	8.0

*Power for these instruments is accounted for by the Signal Conditioner Units.

Table 3 Entry Science Data Summary

Entry Period	Data Format & Bit Rate	VM-8, γ-16°, V_e 4.5 km/sec		VM-2, γ-13.6°, V_e 4.3 km/sec		VM-10, γ-9°, V_e 3.5 km/sec	
		Time (sec)	Data	Time (sec)	Data	Time (sec)	Data
Entry (800,000 ft) to 3000 ft/sec Velocity	Format A, 204 bps	250	61,000 Bits	340	69,360 Bits	410	83,640 Bits
3000 ft/sec Velocity to Aeroshell Staging	Format B, 204 bps	75	15,360 Bits	76	15,504 Bits	210	42,840 Bits
	Television Format, 1 Image/10.4 sec		7 Images		7 Images		20 Images
Aeroshell Staging to 4000 ft Altitude	Format C, 248 bps	20	4,960 Bits	44	10,912 Bits	73	18,104 Bits
	Television Format, 1 Image/10.4 sec		2 Images		4 Images		7 Images
4000 ft Altitude to Landing	Format C, 248 bps	25	6,200 Bits	36	8,928 Bits	25	6,200 Bits
	Television Format, 1 Image/10.4 sec		2 Images		3 Images		2 Images

Table 4 Format A NRT Data Entry (800,000) to 3000 ft/sec Velocity

MEASUREMENT	SAMPLES/ SECOND	BITS/ WORD	WORDS/ MAJOR FRAME	BITS/ MAJOR FRAME	REMARKS
Science Data					
Atmospheric Composition	1/16	7	56	392	Note 1
Modulator Sweep, Mass Spectrometer	1/16	7	56	392	Note 2
*Pressure, Stagnation, (NASA Ames)	1	10	16	160	
*Pressure, Stagnation (Rosemount)	1	10	16	160	
*Acceleration, Longitudinal	1	10	16	160	
*Acceleration, Lateral	1	10	16	160	
*Acceleration, Vertical	1	10	16	160	
Engineering Data					
Science and Power Subsystem					
Temperature, Pressure Stagnation	1/4	7	4	28	
Temperature, Pressure Stagnation	1/4	7	4	28	
Temperature, Acceleration, Long.	1/4	7	4	28	
Temperature, Acceleration, Lat.	1/4	7	4	28	
Temperature, Acceleration, Vert.	1/4	7	4	28	
Temperature SDS Unit	1/4	7	4	28	
Volts, 28 VDC Power Subsystem	1/4	7	4	28	
Current, 28 VDC Power Subsystem	1/4	7	4	28	
Bilevel Event Data (20)	1/4	10	8	80	Note 3
TV power turn on					
Instrument calibrate initiate					
Mass spectrometer sequencing					
T-800,000 ft command					
(Spare Bilevel Channels - 16)					
Spare Data Channels Analog					
4 Data Channels	1	10	64	640	
2 Data Channels	1/4	10	8	80	
4 Data Channels	1/4	7	16	112	
Time Code	1	17	16	272	
Sync Code	1	17	16	272	

BITS/MAJOR FRAME 3264
BITS/MINOR FRAME 204 bps

NOTES

A major frame equals 16 minor frames; minor frame rate is one per second.

*Analog data paralleled for back-up by C/B telemetry.

Note 1: The 56 digital words from the mass spectrometer represent 50-7 bit atmospheric composition words and 6 - 7 bit spectrometer engineering data words.

Note 2: The 56 spectrometer sweep words are 50 - 7 bit sweep calibration words and 6 - 7 bit spectrometer engineering words.

Note 3: 20 bilevel channels of on-off event data (2-10 bit words, each bilevel channel represents 1 bit).

Table 5 Format B NRT Data 3000 ft/second Velocity to Aeroshell Staging

MEASUREMENT	SAMPLES/ SECOND	BITS/ WORD	WORDS/ MAJOR FRAME	BITS/ MAJOR FRAME	REMARKS
Science Data					
*Pressure, Stagnation, (NASA Ames)	1	10	16	160	
*Pressure, Stagnation, (Rosemount)	1	10	16	160	
*Acceleration, Longitudinal	1	10	16	160	
*Acceleration, Lateral	1	10	16	160	
*Acceleration, Vertical	1	10	16	160	
*Temperature, Total	1	10	16	160	
Engineering Data Science and Power Subsystem					
Temperature, Pressure Stagnation	1/4	7	4	28	
Temperature, Pressure Stagnation	1/4	7	4	28	
Temperature, Acceleration, Long.	1/4	7	4	28	
Temperature, Acceleration, Lat.	1/4	7	4	28	
Temperature, Acceleration, Vert.	1/4	7	4	28	
Temperature, SDS Unit	1/4	7	4	28	
Volts, 28 VDC Power Subsystem	1/4	7	4	28	
Current, 28 VDC Power Subsystem	1/4	7	4	28	
Communication Subsystem					
Volts Bias UHF Transmitter 1	1/4	7	4	28	
Volts, Bias UHF Transmitter 2	1/4	7	4	28	
Power output UHF Transmitter 1	1/4	7	4	28	
Power output UHF Transmitter 2	1/4	7	4	28	
Television - Entry					
Current, vidicon filament	1/4	7	4	28	
Video, output, peak detector	1/4	7	4	28	
Current, horizontal deflection	1/4	7	4	28	
Current, vertical deflection	1/4	7	4	28	
Voltage, power supply multivibrator	1/4	7	4	28	
Temperature, vidicon faceplate	1/4	7	4	28	
Iris follow	1/4	7	4	28	
Volts, photometer output	1/4	7	4	28	
Volts, 6.3V regulator	1/4	7	4	28	
Volts, grid regulator	1/4	7	4	28	
Volts, focus regulator	1/4	7	4	28	
Temperature, power conditioner	1/4	7	4	28	
Bilevel Event Data (20)	1/4	10	8	80	Note 1
3000 ft/sec velocity signal Format B data modes UHF Transmitter on Static storage read-out TV frame sequence initiate TV prepare lamp circuit TV wobbler circuit (Spare Bilevel Channels - 13)					
Spare Data Channels Analog					
3 Data Channels	1	10	48	480	
2 Data Channels	1/4	10	8	80	
16 Data Channels	1/4	7	64	448	
Time Code	1	17	16	272	
Sync Code	1	17	16	272	

BITS/MAJOR FRAME 3264
BITS/MINOR FRAME 204 bps

NOTES

A major frame equals 16 minor frames; minor frame rate is one per second.

*Analog science data paralleled for back-up by C/B telemetry.

NOTE 1: 20 bilevel channels of on-off event data (2-10 bit words, each bilevel channel represents 1 bit).

Table 6 Format C NRT Data Aeroshell Staging to Landing + 120 seconds

MEASUREMENT	SAMPLES/ SECOND	BITS/ WORD	WORDS/ MAJOR FRAME	BITS/ MAJOR FRAME	REMARKS
Science Data					
Atmospheric Composition	1/8	7	112	784	Note 1
Modulation Sweep, Mass Spectrometer	1/8	7	112	784	Note 2
*Pressure, Total	1/2	10	8	80	
*Temperature Total	1/2	10	8	80	
*Humidity	1/2	10	8	80	
*Acceleration, Longitudinal	1/2	10	8	80	
*Acceleration, Lateral	1/2	10	8	80	
*Acceleration, Vertical	1/2	10	8	80	
Engineering Data					
Science and Power Subsystem					
Temperature, SDS Unit	1/4	7	4	28	
Temperature, Pressure Total	1/4	7	4	28	
Temperature, Temperature Total	1/4	7	4	28	
Temperature, Humidity	1/4	7	4	28	
Temperature, Accel. Long.	1/4	7	4	28	
Temperature, Accel. Lat.	1/4	7	4	28	
Temperature, Accel. Vert.	1/4	7	4	28	
Volts, 28 VDC Power Subsystem	1/4	7	4	28	
Current, 28 VDC Power Subsystem	1/4	7	4	28	
Communication Subsystem					
Volts, Bias UHF Transmitter 1	1/4	7	4	28	
Volts, Bias UHF Transmitter 2	1/4	7	4	28	
Power Output UHF Transmitter 1	1/4	7	4	28	
Power Output UHF Transmitter 2	1/4	7	4	28	
Television - TDL					
Current, Vidicon filament	1/4	7	4	28	
Video output, peak detector	1/4	7	4	28	
Current, horizontal deflection	1/4	7	4	28	
Current, vertical deflection	1/4	7	4	28	
Voltage, power supply multivibrator	1/4	7	4	28	
Temperature, vidicon faceplate	1/4	7	4	28	
Iris follow	1/4	7	4	28	
Volts, photometer output	1/4	7	4	28	
Volts, 6.3V regulator	1/4	7	4	28	
Volts, grid regulator	1/4	7	4	28	
Volts, focus regulator	1/4	7	4	28	
Temperature, power conditioner	1/4	7	4	28	
Bilevel Event Data (20)	1/4	10	8	80	Note 3
Aeroshell separate signal					
Format C data mode					
Static storage read-out					
TV frame sequence initiate					
Vernier start command					
Vernier shut-down command					
Mass spectrometer initiate					
TV prepare lamp circuit					
TV wobbler circuit					
TV lens cap position					
(Spare Bilevel Channels - 10)					
Spare Data Channels Analog					
7 Data channels	1/2	10	56	560	
3 Data channels	1/4	7	12	84	
Time Code	1	14	16	224	
Sync Code	1	17	16	272	

BITS/MAJOR FRAME 3968
BITS/MINOR FRAME 248 bps

NOTES

A major frame equals 16 minor frames; minor frame rate is one per second.

*Analog science data paralleled for back-up by C/B Telemetry.

Note 1: The 112 digital words from the mass spectrometer represent 100-7 bit atmospheric composition words and 12-7 bit spectrometer engineering data words.

Note 2: The 112 spectrometer sweep words are 100-7 bit sweep calibration words and 12-7 bit spectrometer engineering words.

Note 3: 20 bilevel channels of on-off event data (2-10 bit words, each bilevel channel represents 1 bit).

Table 7 Real Time Format - Television

MEASUREMENT	BITS/ SAMPLE	SAMPLES/ SECOND	BITS/ SECOND	REMARKS
Television Image Line	1440			240 horizontal elements per TV line digitized to 6 bit/element
Identification, Camera	3			
Identification, TV Frame	6			
Identification, TV line	9			
Time Code	12			
Sync Code, pseudorandom	30			
BITS/TV MINOR FRAME	1500	1/60MS		One complete TV scan line